



FACILITY FORM 608

N64-32897

(ACCESSION NUMBER)

47

(PAGES)

CR 57016

(NASA CR OR TMX OR AD NUMBER)

(THRU)

(CODE)

(CATEGORY)

## AN EXPLORATORY STUDY OF SIMULATION OF LIQUID IMPACT IN SPACE VEHICLE AND BOOSTER TANKS

BY

JOHN F. DALZELL  
LUIS R. GARZA

### OTS PRICE

XEROX

\$ 2.00 *per*

MICROFILM

\$ 50 *mf*

TECHNICAL REPORT NO. 9  
CONTRACT NO. NAS 8-1555  
SWRI PROJECT NO. 02-1072

PREPARED FOR

NATIONAL AERONAUTICS AND SPACE ADMINISTRATION  
GEORGE C. MARSHALL SPACE FLIGHT CENTER  
HUNTSVILLE, ALABAMA

SEPTEMBER 1964

**SOUTHWEST RESEARCH INSTITUTE**  
SAN ANTONIO HOUSTON

SOUTHWEST RESEARCH INSTITUTE  
8500 Culebra Road, San Antonio, Texas 78206

Department of Mechanical Sciences

AN EXPLORATORY STUDY OF SIMULATION OF LIQUID  
IMPACT IN SPACE VEHICLE AND BOOSTER TANKS

by

John F. Dalzell  
Luis R. Garza


Technical Report No. 9  
Contract No. NAS8-1555  
SwRI Project No. 02-1072

Prepared for

National Aeronautics and Space Administration  
George C. Marshall Space Flight Center  
Huntsville, Alabama

September 1964

APPROVED:



---

H. Norman Abramson, Director  
Department of Mechanical Sciences

## SUMMARY

32897

This report summarizes exploratory work oriented toward the general problem of liquid impact in space vehicle and booster tanks. In part the work involved putting back in operation the impact test facility previously used in earlier work conducted for the Army Ballistic Missile Agency. General fluid impact simulation studies were carried out with the conclusion that while fluid simulation for the launch abort case is possible in selected circumstances it is doubtful that simulation can be attained for every conceivable case. Similarly successful simulation of the general low gravity case in the laboratory is doubtful though apparently possible in particular instances. Since it does not appear possible to eliminate fluid scale effects in very many cases by experimental design, the magnitude of scale effect must be established. To this end a series of experiments to check for viscous and surface tension scale effects was planned and partially carried out on the fluid impact facility.

The results indicate that a serious viscous scale effect may exist, but this indication must be further verified since the quality of the initial experimental design and of the data was not all that one could desire. The existing fluid impact facility suffers from lack of flexibility in total acceleration stroke and in lack of control over the pulse shape. Recommendations for further study include development of a better definition of the most pressing problem areas, a better theoretical understanding of the fluid motion, prior to and during impact, and serious consideration of new impact facilities if the scale effect investigations are to be continued.

A handwritten signature in dark ink, appearing to read "H. A. ...", is written diagonally across the bottom right of the page.

## TABLE OF CONTENTS

	Page
LIST OF ILLUSTRATIONS	iv
NOMENCLATURE	v
I. INTRODUCTION	1
II. ANALYSIS	2
II. 1 General Simulation Theory	2
II. 2 Application to Abort during Launch	8
II. 3 Simulation of Liquid Impact under Low Gravity	11
II. 4 Summary of Simulation Study	12
III. EXPERIMENTAL PROGRAM	14
III. 1 Experimental Procedure	14
III. 2 Experimental Results	16
III. 3 Discussion	18
III. 4 Summary of Experiments	20
IV. RECOMMENDATIONS	21
V. REFERENCES	22

## LIST OF ILLUSTRATIONS

<u>Figure</u>		<u>Page</u>
1	Approximate Simulation Ranges	23
2	Simulation Plot, Prototype Liquid; Liquid Hydrogen	24
3	Simulation Plot, Prototype Liquid; Liquid Oxygen	25
4	Simulation Plot, Prototype Liquid; Water	26
5	Simulation Plot, Prototype Liquid; Hydrogen Peroxide	27
6	Simulation Plot, Prototype Liquid; White Fuming Nitric Acid	28
7	Simulation Plot, Prototype Liquid; JP-4	29
8	Simulation Plot, Prototype Liquid; Kerosene	30
9	Test Facility	31
10	Tank and Associated Force Balance	32
11	Typical Test Record Expanded to Engineering Units	33
12	Normalized Acceleration Pulses	34
13	Normalized Initial Impact Forces, Test Fluid: Water	35
14	Normalized Initial Impact Forces, Test Fluid: 30% Glycerol	36
15	Normalized Initial Impact Forces, Test Fluid: Methyl Alcohol	37
16	Model and Prototype "Reynolds" and "Weber" Number Ranges	38
17	Comparisons with Previous Impact Data	39

## NOMENCLATURE

$a$	Acceleration, general
$a_d$	Acceleration due to drag
$a_r$	Acceleration ratio
$a_t$	Acceleration due to thrust
$D$	Rocket vehicle drag
$d$	Tank diameter
$F$	Liquid impact force
$F_r$	Force ratio
$g$	Standard gravity
$h$	Test facility acceleration stroke
$L$	Characteristic length
$L_p$	Prototype length
$L_m$	Model length
$M$	Rocket mass
$n_s$	$2h/g T_m^2$
$P$	Pressure
$P_r$	Pressure ratio
$\underline{R}$	A "Reynolds" type parameter
$T$	Time, general
$T_m$	Model time

# NOMENCLATURE (cont'd)

$T_s$	Duration of test acceleration stroke
$T_p$	Prototype time
$\bar{T}$	Rocket thrust
$t$	Time
$V$	Total tank volume
$W(t)$	Vehicle weight (terms of sea level gravity)
$\underline{W}$	A "Weber" type parameter
$\alpha$	Fraction of tank volume occupied by liquid
$\theta_r$	Contact angle ratio
$\theta$	Contact angle
$\lambda$	Geometric scale ratio ( $=L_m / L_p$ )
$\mu_g$	Gas viscosity
$\mu_l$	Liquid viscosity
$(\mu_g)_r$	Gas viscosity ratio
$(\mu_l)_r$	Liquid viscosity ratio
$\nu$	Liquid kinematic viscosity
$\rho_g$	Gas mass density
$\rho_l$	Liquid mass density
$(\rho_g)_r$	Gas mass density ratio
$(\rho_l)_r$	Liquid mass density ratio
$\rho_r$	Density ratio

## NOMENCLATURE (cont'd)

$\sigma_{lg}$  Surface tension

$(\sigma_{lg})_r$  Surface tension ratio

$\tau$  Time scale ratio ( $=T_m/T_p$ )

$\phi_r$  "Kinematic" surface tension ratio

## I. INTRODUCTION

In the nearly 8 years since the acquisition of the first data on fluid impact in rocket booster tanks, Reference 1 and 2, boosters have grown in size, fuels have become more exotic and missions more exacting. In addition, rupture of fuel or oxydizer tank domes due to fluid impact has been suspected, and the possibility of fluid impact in orbiting space craft has been broached. Consequently it was appropriate to re-open the question of simulation in the laboratory of fluid impact in rocket fuel tanks, and this report summarizes the resulting exploratory investigations.

These investigations were oriented toward no specific flight situation as had been the case in Reference 1, but were aimed at ascertaining how much laboratory simulation with the equipment used in Reference 1 was feasible of a variety of possible flight situations, tank sizes and fuels. The successes of Reference 1 and the indications of Reference 3 on the possibilities of simulating low gravity conditions were encouraging with respect to the eventual success of this exploratory program. However, the removal of flight situation and fluid restrictions, and the inclusion of the greater tank sizes in use or contemplated, worked in the opposite direction and it is not yet possible to say that the special equipment used in Reference 1 will be useful for more than a small fraction of possible impact problems, or for that matter how many situations it is possible to investigate with any terrestrial laboratory equipment. The first few sections of the report summarize the general simulation study, and the remainder of the report presents some data obtained from the initial stages of an ensuing scale effect study.

## II. ANALYSIS

### II. 1 General Simulation Theory

#### II. 1a Dimensional Analysis

Dimensional analyses of the fluid impact problem were carried out in Reference 1 for a rigid tank assuming density and viscosity of liquid and gas and surface tension to be the important fluid variables. Reference 4 is an example of a particularly complete dimensional analysis for fuel sloshing in elastic tanks. This analysis contains many parameters but neglects surface tension. Adding surface tension to the analysis of Reference 4 is simple, but the number of nondimensional modeling ratios in such an analysis is very large. Since it may be shown that the addition of new parameters to a dimensional analysis does not change the nondimensional relationships of the old parameters, it was felt that consideration of elastic tanks could to advantage be carried out after consideration of the rigid tank case. The analysis of Reference 1 considered:

Liquid density	$\rho_l$
Liquid viscosity	$\mu_l$
Gas density	$\rho_g$
Gas viscosity	$\mu_g$
Surface tension	$\sigma_{lg}$
Acceleration	$a$
Time	$T$
Characteristic length	$L$

as parameters and pressure (P) as the dependent variable.

To this list should be added the contact angle ( $\Theta$ ) as a measure of gas-solid and liquid-solid surface "tensions." Additionally compressibilities and liquid vapor pressure could have been added but this addition was deferred.

The ratio notation used in Reference 1 is convenient in modeling:

- a. If  $L_p$  and  $L_m$  are prototype and model characteristic lengths

$$L_r = \lambda = \frac{L_m}{L_p}$$

- b. Similarly for characteristic times,  $T_p$ ,  $T_m$

$$\frac{T_m}{T_p} = \tau = T_r$$

- c. And for other variables the subscript "r" indicates ratio of model to prototype quantities.

The modeling relations are (as in Ref. 1):

<u>Condition</u>	<u>Relations</u>
a. Geometrical similarity	-
b. Pressure ratio	$P_r = (\rho_\ell)_r a_r \lambda$
c. Force ratio	$F_r = (\rho_\ell)_r a_r \lambda^3$
d. Acceleration ratio	$a_r = \lambda / \tau^2$
e. Mass density	$(\rho_\ell)_r = (\rho_g)_r = \rho_r$
f. Viscosity	$(\mu_\ell)_r = (\mu_g)_r$
g. Viscosity	$(\mu_\ell)_r = \lambda^2 \rho_r / \tau$
h. Surface tension	$(\sigma_{\ell g})_r = \rho_r \lambda^3 / \tau^2$
i. Contact angle	$\Theta_r = 1$

Rearranging the equations (d, g, h,) so that  $\lambda$ ,  $\tau$ ,  $a_r$  may be solved for, given the fluid properties:

$$(1) \quad a_r = \frac{\left[ \frac{(\sigma_{\ell g})_r}{\rho_r} \right]^3}{\left[ \frac{(\mu_\ell)_r}{\rho_r} \right]^4} = \frac{(\sigma_{\ell g})_r^3 \rho_r}{(\mu_\ell)_r^4}$$

$$(2) \quad \tau = \frac{[(\mu_l)_R / \rho_R]^3}{[(\sigma_{lg})_R / \rho_R]^2} = \frac{(\mu_l)_R^3}{(\sigma_{lg})_R^2 \rho_R}$$

$$(3) \quad \lambda = \frac{[(\mu_l)_R / \rho_R]^2}{(\sigma_{lg})_R / \rho_R} = \frac{(\mu_l)_R^2}{(\sigma_{lg})_R \rho_R}$$

$$(4) \quad \rho_R = (\rho_l)_R = (\rho_g)_R$$

$$(5) \quad (u_g)_R = (u_l)_R$$

$$(6) \quad \text{Contact angle ratio, } \Theta = 1$$

In this problem, there is no particular prototype; the object is to see how wide a range can be covered. Consequently, everything in the last five equations is a variable, pressure or force being dependent variables.

The previous work (Ref. 1) indicated that gas properties might not be critical. Finding proper model liquids is usually a most difficult problem, and so arbitrarily the plan was adopted of selecting a model liquid, then a range of possible prototype liquids and solving for  $a_R$ ,  $\tau$  and  $\lambda$  using Equations 1, 2, and 3.

## II. 1b Model Liquids

Since viscosity, surface tension, and density vary with temperature primarily, with supposedly little effect of pressure, it was thought worth characterizing model fluids over a range of temperature to see what gains might be possible from testing at a higher system temperature than ambient.

It was found that the variation of fluid properties with temperature should be approximately as follows:

$$(\rho_l)_\phi = (\rho_l)_R \left[ \frac{1 + \alpha R + \beta R^2 + \gamma R^3}{1 + \alpha \phi + \beta \phi^2 + \gamma \phi^3} \right] = (\rho_l)_R g(\phi; R)$$

$$(\mu_l)_\phi = (\mu_l)_R \exp \left\{ B \cdot \left[ \frac{R - \phi}{(X + R)(X + \phi)} \right] \right\}$$

$$(\sigma_{lg})_\phi = (\sigma_{lg})_R \left[ \frac{\phi_c - \phi}{\phi_c - R} \right] [g(\phi; R)]^{2/3}$$

where

- $\phi$  = Temperature, °C
- R = Ref. temperature, °C
- X = 273 °C
- $\phi_c$  = Critical temperature of liquid
- B = Empirical constant
- $\alpha$  = Empirical constant
- $\beta$  = Empirical constant
- $\gamma$  = Empirical constant

Values of the empirical constants can be found for some but not all fluids. The same is true for tabulated values themselves.

Six fluids were chosen on the basis of availability, and the "ball park" validity of the foregoing expressions was verified for:

1. Water
2. Carbon tetrachloride
3. Ethyl alcohol
4. Methyl alcohol
5. Methelene chloride
6. Mercury

In addition, solutions of glycerol and sucrose were added to the list of model fluids. These were taken at 20°C, and instead of varying temperature the percentage of solution was varied within the following ranges:

Glycerol solution: 5-50%  
 Sucrose solution: 20-60%

## II. 1c Prototype Liquids

Since no specification of prototype is given, a reasonable guess at a range of liquids which might be involved is all that can be done. For present purposes the following liquids were presumed:\*

	Liquid	$\rho_l$ (gm/cc)	$\mu_l$ (cp)	$\sigma_l$ g(dynes/cm)
1	Liquid hydrogen	.071	.013	2
2	Liquid oxygen	1.14	.19	13
3	Hydrogen peroxide	1.44	1.25	76
4	JP-4	.78	.83	30**
5	White fuming nitric acid	1.51	0.86	41
6	Kerosene	.83	2.5	28**
7	Water	1.0	1.0	73

\* Data largely from Reference 4.

\*\* Very approximate

## II. 1d Simulation Plots

The question in the present project is primarily what length ( $\lambda$ ) and acceleration ( $a_r$ ) scale ratios can be mechanically simulated with the equipment at our disposal. Presuming solutions for  $a_r$  and  $\lambda$  for specific fluids, a plot of  $a_r$  versus  $\lambda$  would prove useful in showing what can be done.

Given:

$$\lambda = \frac{\mu_r^2}{\sigma_r \rho_r} \qquad a_r = \frac{\sigma_r^3 \rho_r}{4 \mu_r}$$

Consequently:

$$a_r = \frac{1}{\lambda^2} \left( \frac{\sigma_r}{\rho_r} \right) = \frac{1}{\lambda^2} \phi_r \quad (\phi_r = \text{kinematic surface tension ratio})$$

The kinematic surface tension of the assumed prototype liquids ranges from 11.4 to 73, or approximately 10 to 100 (dyne-cm/gm). Kinematic surface tension of model liquids at the reference temperature ranges from 17 to 72, also an approximate range of 10 to 100 (dyne-cm/gm). Thus  $\phi_r$  at reference temperature might range from 0.1 to 10. The expected region on a  $\lambda$ - $a_r$  plot where solutions will be found is bounded by  $(a_r)_{\max} = 10/\lambda^2$  and  $(a_r)_{\min} = 1/10\lambda^2$  (a region on a log-log plot bounded by two straight lines). Variation outside this band is highly unlikely. A further consideration is that scale ratios ( $\lambda$ ) greater than one are probably of very slight practical interest.

Figure 1 is a rough log-log plot of the regions of possible relations between  $a_r$  and  $\lambda$ . A band (unshaded) denotes a region of probable solutions; below this band solutions are faintly possible; above it, probably impossible.

Calculations were made on the GE-225 for  $\lambda$  and acceleration ratio  $a_r$  for all combinations of prototype and model fluids. The results are shown in Figures 2 - 8. Each of these figures pertains to a particular prototype liquid, and simulation possibilities for all of the eight model fluids are shown on each, as is the estimate

$$a_r^i = 1/\lambda^2$$

A casual check of the plots 2 - 3 shows that the approximate simulation range for various fluids hugs the  $a_r = 1/\lambda^2$  curve very closely, and in fact almost all the curves for various fluids are within the "region of probable solutions," Figure 1. Moreover, there is a general tendency for most of the simulation curves to lie in the region where the model is larger than the prototype. In addition, many of the simulation curves

involve model fluids at extremely high temperatures and pressures since calculations for model fluid properties were carried out to within a few degrees of critical temperature in some cases. In general the more viscous the prototype fluid, the more possibilities that exist with scale ratio  $\lambda$  less than 1. When extreme model temperatures are disregarded, relatively few simulation points exist.

## II. 1e Considerations on Geometrical Scale Ratio

The work of the preceding section has shown some possible relationships between various scale ratios but still does not clearly show what can (or cannot) be done with the tank bulkhead impact problem.

Perhaps the simplest scale ratio is  $\lambda$  and it may be useful to put some bounds on it. A perusal of the handbooks indicates that the prototype fluids quoted in the preceding sections may be contained in cylindrical, spherical or toroidal tanks (plus variations on these themes). Typical cylindrical or spherical tank diameters range from 1 to 12 feet for present day rockets up to Saturn class, and contemplations in the handbooks on the Nova class indicate maxima of 16 feet. For orders of magnitude, it might therefore be wise to consider 30-foot diameter tanks as the largest in the foreseeable future.

At the other end of the prototype scale typical tank diameters may range down to 6" or so in space craft. However, at this end of the scale, structural problems should not be of great moment - especially as the prototype size is about equal to model size.

Consequently, the probable range of prototype tank diameters of interest would be from 3 to 30 feet. Some idea of convenient model sizes is necessary. Since a one-foot diameter model is not too cumbersome an object, one foot will be taken as about the upper limit on model size.

For maximum model size,  $\lambda$  becomes 0.33 to 0.033. If we wish to measure pressures, a model diameter of 1/3 foot is probably smaller than convenient. Assuming this dimension for minimum model size results in a scale ratio range from 0.1 to 0.01. Combining the two ranges, geometric scale ratio  $\lambda$  may be expected to have the following extreme practical range:

$$0.01 \leq \lambda \leq 0.3$$

A comparison of this range with the results in Figures 2 - 8 further restricts possible simulation points.

## II. 2 Application to Abort during Launch

What are the magnitudes of accelerations produced by rocket thrust and drag?

### II. 2a Earth Gravitational Field

Since in the abort case we are dealing with the first 100 miles off the earth, the earth's gravitational field may be assumed roughly constant.

### II. 2b Acceleration Due to Thrust

The component of acceleration due to rocket thrust is along the rocket axis and equal to

$$a_t = \bar{T}/M$$

where  $\bar{T}$  = thrust  
 $M$  = rocket mass

Strictly speaking,  $\bar{T}$  varies with altitude and time and  $M$  varies with time as fuel is consumed. The major variation in  $\bar{T}/M$ , however, may be ascribed to mass variation during flight. Thus, holding  $\bar{T}$  constant at the rated engine thrust

$$T/M \approx \frac{Tg}{W(t)} = K_t g$$

$g$  = standard gravity

$W(t)$  = vehicle weight (in terms of sea level gravity)

$K_t$  =  $\bar{T}/W(t)$

Some rough figures on typical values of  $K_t$  can be obtained from Reference 6 taking quoted design weights and thrusts and computing minimum  $K_t$  for the case of full fuel load and maximum  $K_t$  for the case of almost exhausted fuel. Typical results are as follows:

Rocket	Lift Off	First Stage Cut Off	Second Stage Ignition	Second Stage Cut Off
Thor Agena B	1.34	7	1.07	6
Atlas Agena A	1.31	14	1.55	3.5
Saturn C 1	1.30	3.7	0.63	2
Nova	1.34	3.2	0.65	1.15

It appears that acceleration due to thrust will vary from about 1 to 10 g's. Probably a narrower range (1→5g) would be appropriate for manned missions.

## II. 2c Acceleration Due to Drag

Some order-of-magnitude estimates of drag from Reference 6 result in values varying from nearly nothing to (.3) times thrust at the outside for the rocket vehicles cited previously.

Since the acceleration magnitude due to drag will be:  $a_d = D/M$   
Substituting  $D = K_d T$  and  $\bar{T}/W(t)$ :

$$a_d = \frac{\bar{T}}{W(t)} K_d g = K_t K_d g$$

Summary of order-of-magnitude estimates for thrust, drag, and gravitational acceleration:

$$a_g = g$$

$$a_t = K_t g$$

$$a_d = K_t K_d g$$

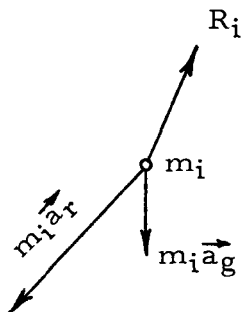
$$1 < K_t < 10$$

$$0 < K_d < .3$$

The thrust and drag accelerations can be assumed along the axis of the rocket.

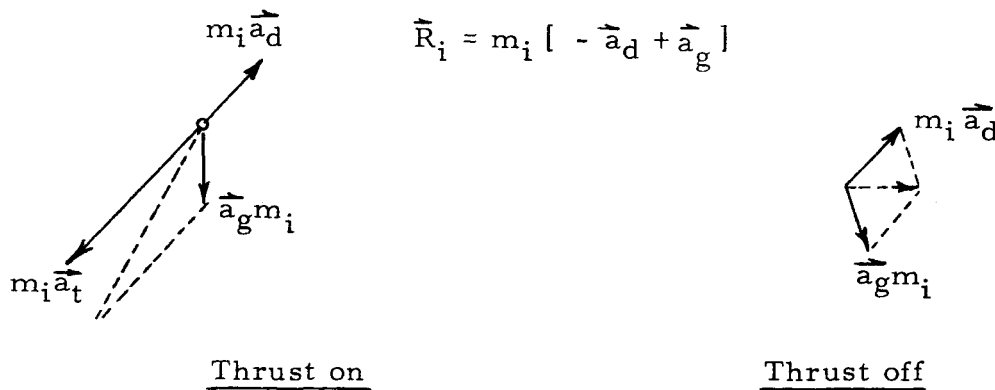
## II. 2d Simulation of Net Acceleration

The net reaction on each particle of fluid if attached to the tank is the vector sum of its mass times gravitational acceleration plus the negative of the rocket's axial acceleration.



$$\begin{aligned} \vec{R}_i &= m_i [ \vec{a}_r + \vec{a}_g ] \\ &= m_i [ \vec{a}_t - \vec{a}_d + \vec{a}_g ] \end{aligned}$$

When the thrust is cut off



It can be seen that cutting off thrust is equivalent to suddenly altering the magnitude of and rotating an effective gravitational field. When the angle between earth gravity and the rocket axis is small, the magnitude of the effective gravitational field becomes

$$|\vec{a}_r + \vec{a}_g| \approx g [K_t - K_t K_d + 1]$$

The value of this expression ranges from 1.7 to 11 g.

After the thrust is cut

$$|\vec{a}_r + \vec{a}_g| \approx [-K_t K_d + 1]g$$

(for small angle between earth gravity and rocket axis).

The value of the last expression ranges from +g to -2g. If the equilibrium acceleration before the abort is simulated by 1g in the laboratory (a model tank standing still) we must have an acceleration scale ratio less than 1. Unfortunately, acceleration ratios less than 1 and geometric scale ratios from .01 to .3 are in a region on the fluid simulation plots Figures 2 - 8 where full viscous and surface tension scaling is extremely unlikely. It will consequently be impossible to simulate the initial acceleration conditions with 1g in the laboratory. Hope of simulation of the abort lies in the region of acceleration scale ratio greater than 1.

How could the initial conditions of the abort be simulated for acceleration scale ratios greater than one? One possibility would be to accelerate a sled toward the ground with small rockets, then cut off and decelerate. The powered part of the ride would have to be sufficiently long so that equilibrium conditions would be reached. After cutoff, the tank could be made to experience deceleration to simulate conditions after

prototype thrust cutoff. This scheme would appear to have drawbacks in that while acceleration scale ratios  $> 1$  would be feasible, it is questionable if high enough model accelerations could be maintained to put the acceleration scale ratios up near where fluid simulation seems at all feasible. (For example, a 5g prototype initial acceleration implies 100g model acceleration for an acceleration scale ratio of 20, which is not particularly high as far as fluid simulation is concerned.)

In summary, simulation of both initial and final acceleration conditions for the general abort case does not appear encouraging. The approach used in the past (Ref. 1) was to neglect the initial conditions and simulate the change in acceleration only. This approach implies neglect of lower bulkhead elastic effects, the fluid being assumed incompressible. Simulation of acceleration change on the equipment of Reference 1 is fairly straightforward. Acceleration scale ratios based on change of acceleration range from about 5 to 50 (corresponding to prototype accelerations of 10 to 1g respectively), and these values are at least in the ball park as far as simulation of some prototype fluids is concerned.

It can be seen from the fluid simulation plots Figures 2 - 8, that about the only simulation of fuels which is easy is that which was done in Reference 1 (kerosene with scale ratios  $\approx 0.1$  and acceleration ratios  $\approx 75$ ).

It appears that the simulation equipment of Reference 1 may have rather limited simulation capability, not because of limitations in equipment, but because of limitations on our ability to select fluids suitable for inertial, viscous and surface tension scaling.

### II. 3 Simulation of Liquid Impact under Low Gravity

The existence of some potential fluid simulation points at acceleration scale ratios of  $10^2$  to  $10^3$  on Figures 2 - 8, suggests that low gravity may be simulated at 1g in the laboratory under certain circumstances. In the fluid impact problem, it is not too hard to imagine an orbital rendezvous maneuver with an initial effective acceleration of  $10^{-2}$  or  $10^{-3}$  g and then a sudden deceleration as contact between two orbiting vehicles is made. Initially, fluid in a partially full tank would be gathered at one end and, depending on the magnitude of the deceleration, would move to the other end with resulting impact.

In this case, the potential geometric scale ratio range of interest remains the same, but acceleration ratios  $> 10^2$  would be the acceleration scale range of interest, since the low gravity prototype environment could

be simulated in the laboratory at 1g. Some hope of simulation with very small models is shown in Figures 4 - 8 for water and more viscous fuels, bearing out the indications of Reference 3.

## II. 4 Summary of Simulation Study

### II. 4a General

Assuming both viscosity and surface tension to be important in simulation, very little of the interesting range of geometric and acceleration scale ratios is touched with known fluids, even a smaller to vanishing part if model fluid temperatures are restricted to ambient. The inclusion of mercury as a model fluid and the results indicate the possibility of exploring liquid metals further, especially for low gravity simulation, although sheer model weight would be multiplied manyfold. It is shown that previous simulation successes were largely due to a particularly advantageous problem. How far our general capability at simulating fluid impact problems can be developed remains in question.

It must also be pointed out that present equipment does not have the capability of rotating the apparent gravitational field. This effectively limits its utility to cases where the rocket axis is aligned at small angles to a gravitational field, or to those cases where initial acceleration conditions may be disregarded.

The disparity between what can be done and the general ranges of interest outlined herein is so great that the problem specification should be better defined.

The limitations on our ability to simulate the fluid impact problem, which are pointed out in the foregoing, rest on the hypothesis that liquid density, viscosity and surface tension are the only fluid properties of importance. What other factors are of importance becomes somewhat academic until the validity of the above hypothesis is discarded. It therefore seemed appropriate to initiate an experimental study to ascertain if liquid viscosity and surface tension were, in fact, important, and the plans for such a study are outlined in the next section.

### II. 4b Experimental Plans

The interest lies in maximum impact pressures or forces on the tank dome and the question is how significant to these forces or pressures is variation of liquid surface tension and viscosity.

As is normal to such studies, a series of two or three geometrically similar tanks was envisioned, each to contain liquids of varying viscosity and surface tension. In such a study, an index pressure or force is all that is required. In view of the existing facility (Ref. 1), it was felt wise to plan for two tanks capable of being fitted on the existing facility, one the largest that could be handled, one the smallest which could be instrumented. The instrumentation requirement on the small tank indicated that total dome force could be the most convenient index of dome impact pressures. A third tank, considerably larger with a new low acceleration impact facility, could also be envisioned should studies of the tanks capable of being tested on the existing facility turn up some serious scale effect.

Though full implementation of such a program was beyond the scope of the present program, it was felt possible to proceed with preliminary tests of the largest tank which could be handled on the facility (11" diameter).

It was planned to accelerate this tank over a range of accelerations normal to the initial free surface for each of the following three fluids:

- a. 30% Glycerol solution
- b. Water
- c. Methyl alcohol

It appeared that these tests alone should show scale effect if it was serious in accordance with the scaling relations of the previous section. For example, if it was desired to model the 11-inch tank containing 30% glycerol, these scaling ratios show that a  $1/6$  scale tank and an acceleration scale ratio of 37 would be required if water were the model fluid. Similarly, to model the 11-inch tank containing 30% glycerol solution with methyl alcohol, a  $1/4$  scale tank and acceleration scale ratio of 7.4 would be required.

### III. EXPERIMENTAL PROGRAM

#### III. 1 Experimental Procedure

##### III. 1a Test Facility

The fluid impact test facility which was built some eight years ago at SwRI, was overhauled and installed in a new laboratory space. A general view of the installed facility is seen in Figure 9. The design of this apparatus is covered in some detail in Reference 1, and was used in much the same manner in this series of experiments. In principle, the apparatus consists of a long, pneumatic cylinder and piston rod. The test tank is attached to the end of the piston rod and the assembly is accelerated by high pressure nitrogen over a fixed distance and then decelerated by means of a floating piston in the lower half of the cylinder.

##### III. 1b Tank Design

Certain features of the test apparatus indicated the advisability of designing the tank to have a conical bottom. In line with current practice, it was felt that the upper tank bulkhead should be either ellipsoidal or hemispherical. The ellipsoidal shape was selected arbitrarily. Figure 10 indicates the proportions of the tank.

##### III. 1c Instrumentation

Since it was determined to measure only total force on the upper bulkhead, the ellipsoidal head was fabricated separately from the cylindrical tank body and attached to it through an eight-arm force balance specially built for this project. The eight arms of the force balance (Fig. 10) were fitted with strain gages so that total vertical force on the tank dome could be read out. Since the previous work, Reference 1, indicated that the facility would destroy commercial unbonded strain gage accelerometers in short order, a new bonded strain gage accelerometer was fabricated. Preliminary test findings indicated that the noise level on the accelerometer and force outputs would be extremely high. Consequently, low pass electronic filters were employed to make the records intelligible. Transient response calculations were made for the accelerometer plus filter combination and these indicated that the accelerometer-filter system had a rise time of about 3 milliseconds and a maximum overshoot in response to a step of about 10%. The transient characteristics were felt to be acceptable for acceleration pulse records of total duration from 60 to 200 milliseconds.

The dynamic characteristics of the force balance and the low pass filter employed in conjunction were such that the rise time and overshoot in the force balance would have been less than that for the accelerometer, but detailed calculations were not carried out. The accelerometer was both statically and dynamically calibrated prior to testing. The force balance was statically calibrated prior to the test. In both cases electronic calibration signals were employed to guard against amplifier drift.

### III. 1d Experiments

The first experiments on the 11-inch tank were carried out with an amount of water equivalent to 25% of the total tank volume. In these first tests no fluid force pulse was recorded up to an acceleration pulse magnitude of 4 or 5 g's since the stroke of the apparatus was too short. The experiments were repeated for tank fluid level equivalent to 50% of the tank volume with very much the same results and finally, the tank was filled to a level corresponding to 78% by volume and the remaining experiments carried out with the tank fluid at this level. The acceleration and force time histories were recorded on a dual-trace oscilloscope and photographed, using a standard oscilloscope camera. The raw test data, when expanded to engineering units, was similar to the sketch of Figure 11. The top time history in this figure is that of the force, and the lower that of acceleration. It was noted on all traces that appreciable force due to acceleration of the tank dome was recorded.

In all, three test series were carried out. In each one, the tank orientation to the vertical was  $0^\circ$ , the fluid level in the tank corresponded to the 78% full condition, and the facility acceleration pressure was varied so as to yield acceleration pulse magnitude, varying from 2 or 3 up to 20 g's. In the first test series, water was used as the test fluid. In the second series, a 30% glycerol solution was employed, and in the third test series, methyl alcohol was used.

### III. 1e Data Reduction

Due to the shape of the force pulse shown in Figure 11, it was necessary to make an inertia correction as indicated graphically in the figure. Unfortunately, the resolution on the oscilloscope pictures and the magnitude of the inertia corrections were such that the accuracy of the net fluid impulse forces was seriously degraded.

### III. 2 Experimental Results

#### III. 2a Accelerations

Since the acceleration pulses were neither exactly rectangular or other simple shape, it was decided to characterize the magnitude of the pulse by a function of the uniform acceleration necessary for the tank to travel the constant stroke of the apparatus in the observed time. This acceleration divided by  $g$  is called  $n_s$  and is given by

$$n_s = \frac{2h}{gT_s^2}$$

where  $h$  = stroke of apparatus

$T_s$  = total duration of stroke

This acceleration is inclusive of gravity, and the magnitude of the recorded acceleration pulse was characterized by  $(n_s - 1)$ .

In order to compare the acceleration pulses for different acceleration magnitudes, all of the pulse time histories were normalized. The time scale in each pulse was divided by the total duration of the pulse ( $T_s$ ) and the recorded pulse amplitude was divided by  $(n_s - 1)$ . The results from 45 tests were superimposed. All of these pulse time histories fell within the shaded band in Figure 12. This figure indicates the nature of the acceleration pulse obtainable in this facility for the tank accelerations from 4 to 20g's. Acceleration pulses, whose magnitude was below about 3g's, deviated widely from this form and the few runs obtained at these low acceleration levels were not further analyzed. It is probable that friction in the apparatus prevents adequate control of the acceleration pulse magnitude for less than 3g accelerations.

#### III. 2b Impact Forces

The raw force pulse time histories obtained in these experiments were grossly deficient in that no maximum was reached prior to the end of the acceleration pulse. (Fig. 11 is typical of the better records.) This was a consequence of limited stroke of the facility. It was determined, however, to make as careful as possible a correlation of the initial portion of the force pulse. If viscous and surface tension effects are not important, then the force should non-dimensionalize in a form similar to

$$\frac{F}{\rho a V a}$$

where  $\rho$  is mass density of liquid

$a$  is an acceleration magnitude

$Va$  is the total fluid volume or other geometrical parameter having length cubed dimensions.

$V$  is tank volume

$\alpha$  is fraction of tank volume occupied by fluid

Similarly, assuming neither viscosity nor surface tension to be important, the time scale should non-dimensionalize as follows

$$t \sqrt{\frac{a}{d}}$$

where

$t$  is time

$d$  is tank diameter

The resulting time parameter is analogous to the distance which a free particle falls under the influence of a constant acceleration.

Considerable effort in correlating the 45 force pulse records was expended, and it was found that the best correlation of these time histories was obtained by plotting  $F/\rho g Va(n_s - 1)$  against  $t\sqrt{g(n_s - 1)/d}$ . The acceleration term in each of these parameters is an approximation to the net relative acceleration between a fluid particle in free fall and the accelerated tank. The results are shown in Figures 13, 14 and 15, for water, 30% glycerol and methyl alcohol, respectively. As can be noted, these figures show very few results explicitly. The wide black mean line shown is a line which could represent all of the test data when the test tolerance resulting from the poor resolution of the basic loads is considered. The two outer lines enclosing this black line indicate the spread of normalized time histories. In Figure 15 for methyl alcohol, the heavy black median line has been grossly expanded near its end, this reflecting the non-systematic dispersion between four runs at acceleration levels from 13 to 19g's where the resolution tolerance was relatively small. In Figures 14 and 15, the dashed lines represent an actual force pulse which could not be correlated with the others. Both of these isolated results were at rather low levels of acceleration.

### III. 3 Discussion

#### III. 3a General

A comparison of the magnitude of the force pulses at equivalent normalized times in Figures 13, 14 and 15 shows that the results for water and for methyl alcohol are sufficiently close together so that any differences between impact forces are more than obscured by the general lack of precision in the experiment. However, a comparison of either the water or the methyl alcohol experiments with the results of the 30% glycerol solution, show that the impact forces for the more viscous fluid seem to be almost twice as great as those for the water or alcohol and on the average that the fluid reached the tank dome slightly sooner. In the absence of any realistic analytical treatment of the motion of the fluid, it is difficult to advance reasons for this result. If this result can be verified, it means that a fairly serious viscous scale effect exists. From the practical point of view, even though a viscous scale effect may exist for the initial portions of the force pulse, it may not be serious for maximum force. It must be mentioned that this indication of scale effect is not in agreement with privately communicated preliminary results from NASA Langley, for experiments wherein force maxima were observed.

The importance of the existence or non-existence of a viscous scale effect in small scale experiments may be illustrated as follows.

One of the enormous number of "Reynolds Type" parameters relating the ratio of viscous to inertial forces can be written as follows

$$R = \frac{(n_s - 1)gd^3}{\nu^2}$$

where

$\nu$  is the liquid kinematic viscosity

This "Reynolds Number" can be evaluated approximately for possible prototype tanks as well as the present experiments. The results are shown in graphical form in Figure 16. It is seen that the variation in "Reynolds Number" in the present experiments has spanned almost an order of magnitude. This would be rather exceptional if it were not for the fact that even when one considers kerosene as the prototype liquid in tanks 10 to 30 ft in diameter, an additional 3 orders of magnitude extrapolation is required. If liquid oxygen is assumed, in 10 to 30 ft-diameter tanks, almost 5 orders of magnitude extrapolation from the present experiments is required. Figure 16 also shows that the viscous scale effect indicated by Figures 13 - 15 is plausible since the "Reynolds Number"

ranges for water and alcohol are fairly close together while that for the glycerol solution is half an order of magnitude lower.

An additional nondimensional parameter of interest is one expressing the ratio of inertial to surface tension forces. One of a large number of such parameters is

$$\underline{W} = \frac{(n_s - 1)gd^2}{\phi}$$

where

$\phi$  is the "kinematic" surface tension ( $\sigma/\rho$ )

The upper part of Figure 16 shows similar ranges of this parameter for the present experiments and for large prototype tanks.

Suffice to say the extrapolation problem is sizable for both surface tension and viscosity.

The primary deficiency in the current experiments was that of having failed to achieve a maximum force as was done in Reference 1. It happens that the mean distance through which a fluid particle on the surface had to "fall" in these experiments in order to impact the dome was about  $d/2$ , and thus the numerical value of the time parameter in Figures 13 - 15 is quite reasonable. It is obvious that duration of acceleration pulse will have considerable bearing on test results. So far as simulation is concerned, some rough calculations indicate in the case of prototype launch abort that the time parameter  $t\sqrt{a/d}$  may vary from 1 to 50 thus further complicating the problem.

### III. 3b Comparisons with Previous Data

Only two sources of similar data are available. The first, in chronological order, is that obtained in Reference 1 at SwRI. The data contained in this reference are in the form of pressures instead of total forces on tanks with various head shapes. Two sets of experiments are of interest for comparison, both experiments with the facility orientation at  $0^\circ$  to vertical. One experiment was for a 50% full tank, the other for a 25% full tank. In both these cases, the tank had a head or dome composed of a spherical segment. A fairly crude pressure integration was carried out on the basic data contained in Reference 1, for peak forces, and the results were normalized and are plotted in Figure 17. Privately communicated preliminary data from NASA Langley for total force on the head of a tank having a hemispherical head plot in the shaded range

on this figure. As can be noted, the trends of the data from the two sources do not agree, presumably because the acceleration magnitudes are vastly different. It must also be remarked that the test methods are quite different and the shape of the acceleration time histories differ as well, though the nature of the fluid motion is qualitatively the same. Since the ordinate on Figure 17 is the same as that on Figures 13, 14 and 15, it can be seen that the present data are very much in line with past data so far as order of magnitude is concerned, but that since no peaks were measured in the present data, this comparison is rather inconclusive.

### III. 4 Summary of Experiments

It was found that the test facility previously constructed is capable of imposing a fairly repeatable acceleration pulse of from 4 to 20g's in magnitude on a payload of approximately 125 lb. This acceleration range can, in all probability, be increased to 4 to 50g's with negligible payload. Below approximately 3g tank acceleration, the pulse shape is irregular and difficult to control. In general, this equipment suffers from lack of flexibility in total acceleration stroke and in control over the pulse shape.

It was found that the acceleration pulse duration is likely to be an extremely important variable in the simulation of tank bulkhead impact. In particular, the preliminary experiments deal with a tank too large for the equipment (11-inch diameter).

A fairly consistent indication that viscous scale effects exist in the tank bulkhead impact problem was observed, though the evidence is extremely scanty.

#### IV. RECOMMENDATIONS

The net result of the exploratory studies described herein has been a large increase in the anticipated magnitude of the general fluid impact simulation problem. Considerable work is recommended on better defining the specifications for those impact problems which are of most pressing importance, or on defining whether or not the general problem is worth sizable development effort. In absence of a definitive answer to the above, continuation of the present line of work is not recommended.

Should the problem become better defined or the general problem become of sufficient importance to justify additional development, some even approximate theory for the mode of motion of the fluid from its initial position to the dome is required. The behavior of the fluid in present experiments was apparently very like the behavior in previous experiments, and this has been shown to be extremely complicated. Additionally, in order to continue the necessary scale effect investigations initiated herein, a larger impact facility, as far as stroke is concerned, is badly needed, though such a facility need not have the extremely high acceleration capability of the present equipment.

## V. REFERENCES

1. Epperson, Thomas B., and Brown, Robinson, "Dynamic Loads Due to Fuel Motion in Fuel Tanks of Missiles," Final Report Contract No. DA-23-072-ORD-1062, Southwest Research Institute, June 1957.
2. Epperson, T. B., Brown, R. B., and Abramson, H. N., PROCEEDINGS OF THE FOURTH SYMPOSIUM ON BALLISTIC MISSILE AND SPACE TECHNOLOGY, "Dynamic Loads Resulting from Fuel Motion in Missile Tanks," Volume II, Pergamon Press, New York, 1961.
3. Squire, William S., "Some Preliminary Notes on the Behavior of Liquids Under Conditions of Low Gravity," Southwest Research Institute, March 1960.
4. Sandorff, Paul E., "Principles of Design of Dynamically Similar Models for Large Propellant Tanks," Technical Note D-99, National Aeronautics and Space Administration, January 1960.
5. "Simulation of Fuel Sloshing Characteristics in Missile Tanks By Use of Small Models," by H. Norman Abramson and Guido E. Ransleben, Jr., Tech. Rept. No. 7, April 1960 (also, ARS Journal, 30, pp. 603-612, July 1960).
6. HANDBOOK OF ASTRONAUTICAL ENGINEERING, 1st Edition, McGraw-Hill Book Company, Inc., New York, New York (1961).

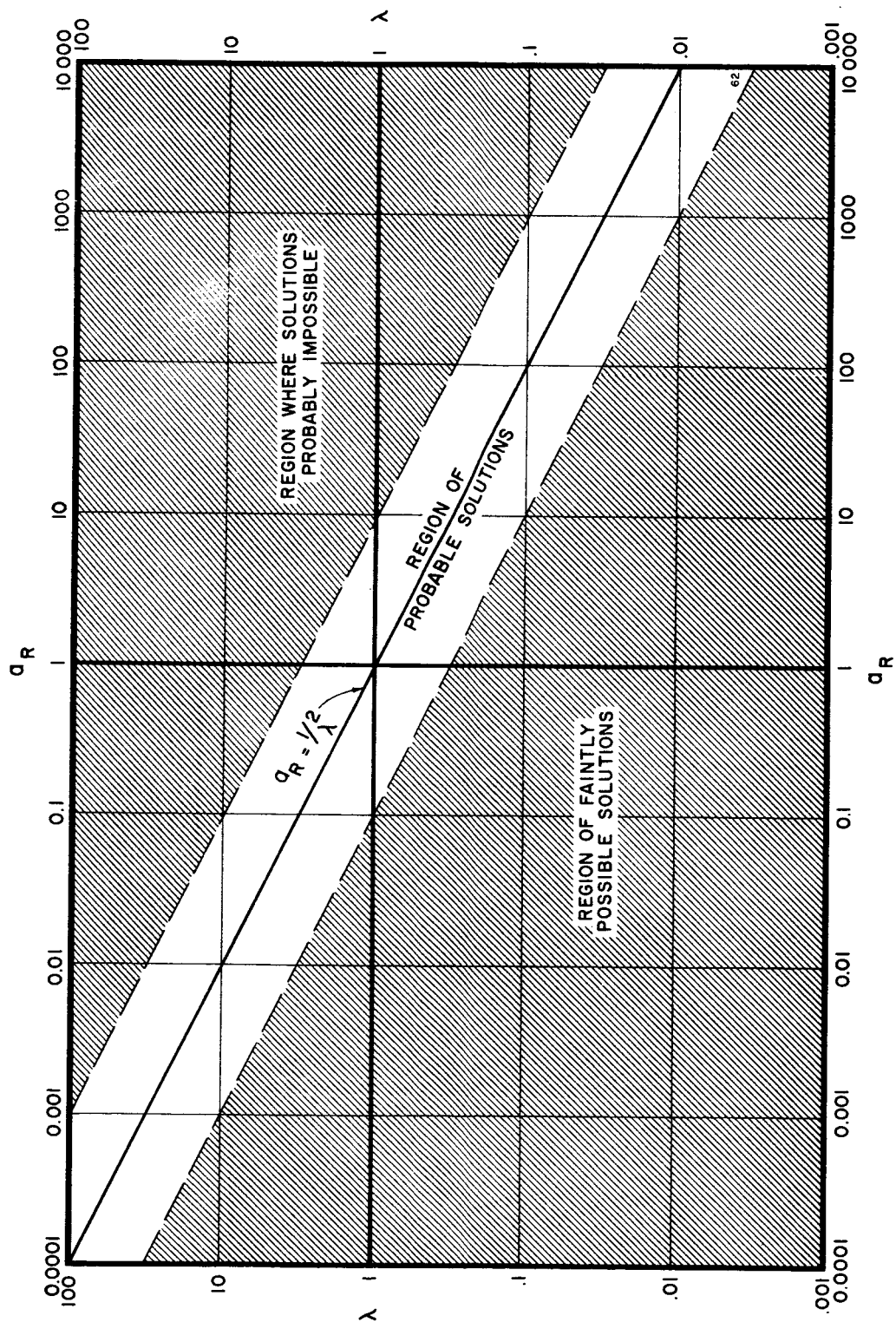


FIGURE 1. APPROXIMATE SIMULATION RANGES

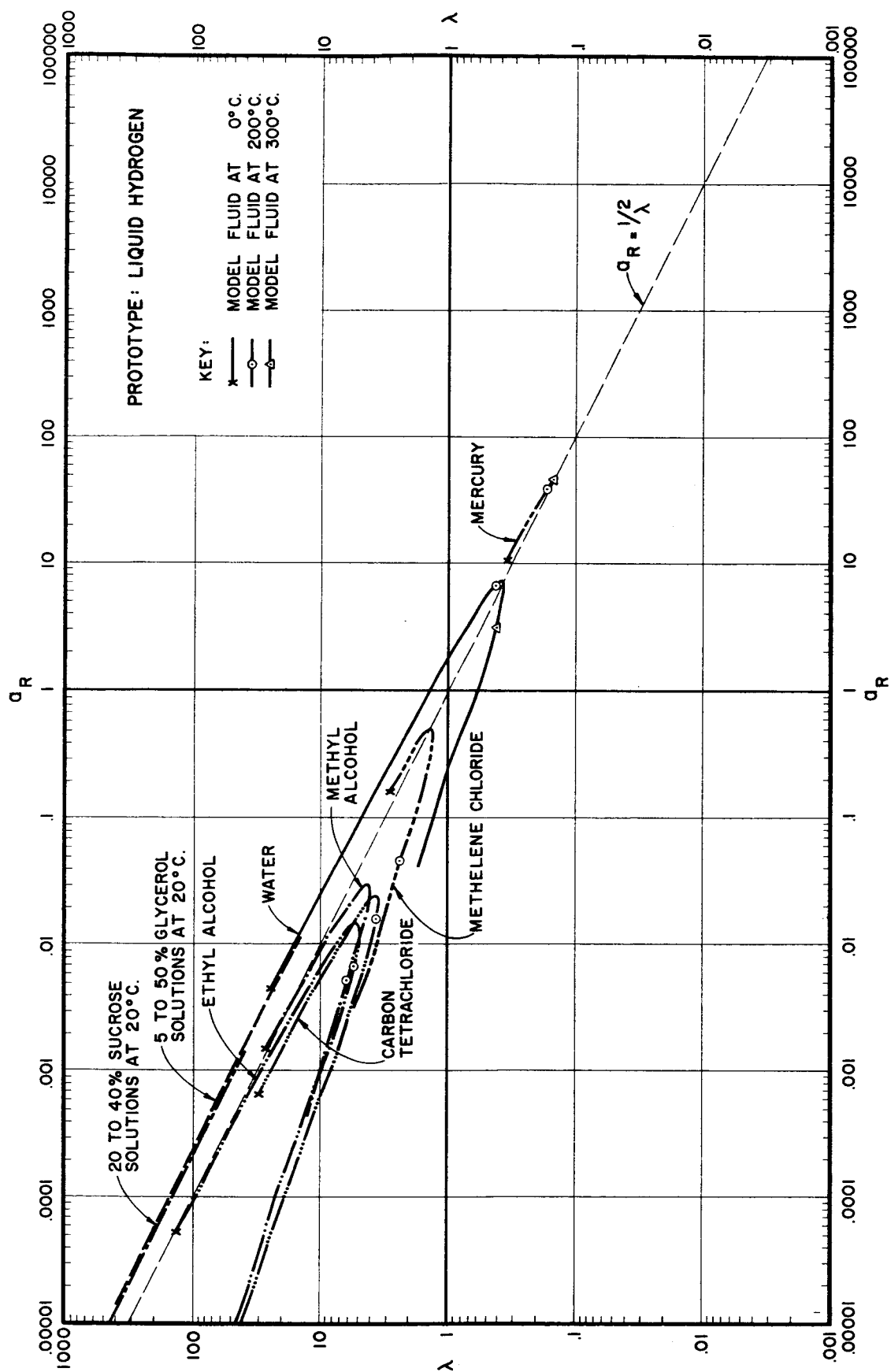


FIGURE 2, SIMULATION PLOT, PROTOTYPE LIQUID; LIQUID HYDROGEN

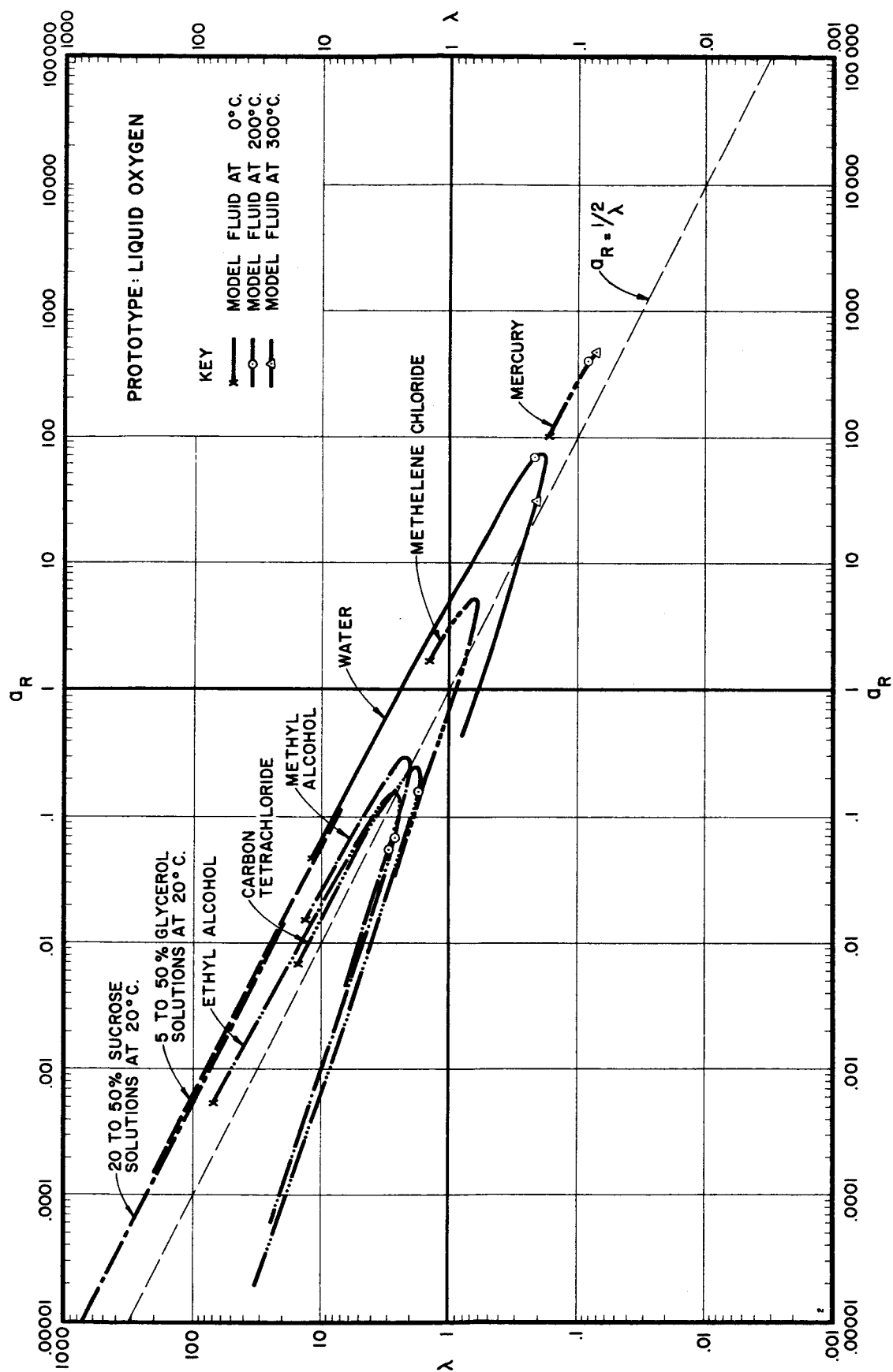


FIGURE 3. SIMULATION PLOT, PROTOTYPE LIQUID; LIQUID OXYGEN

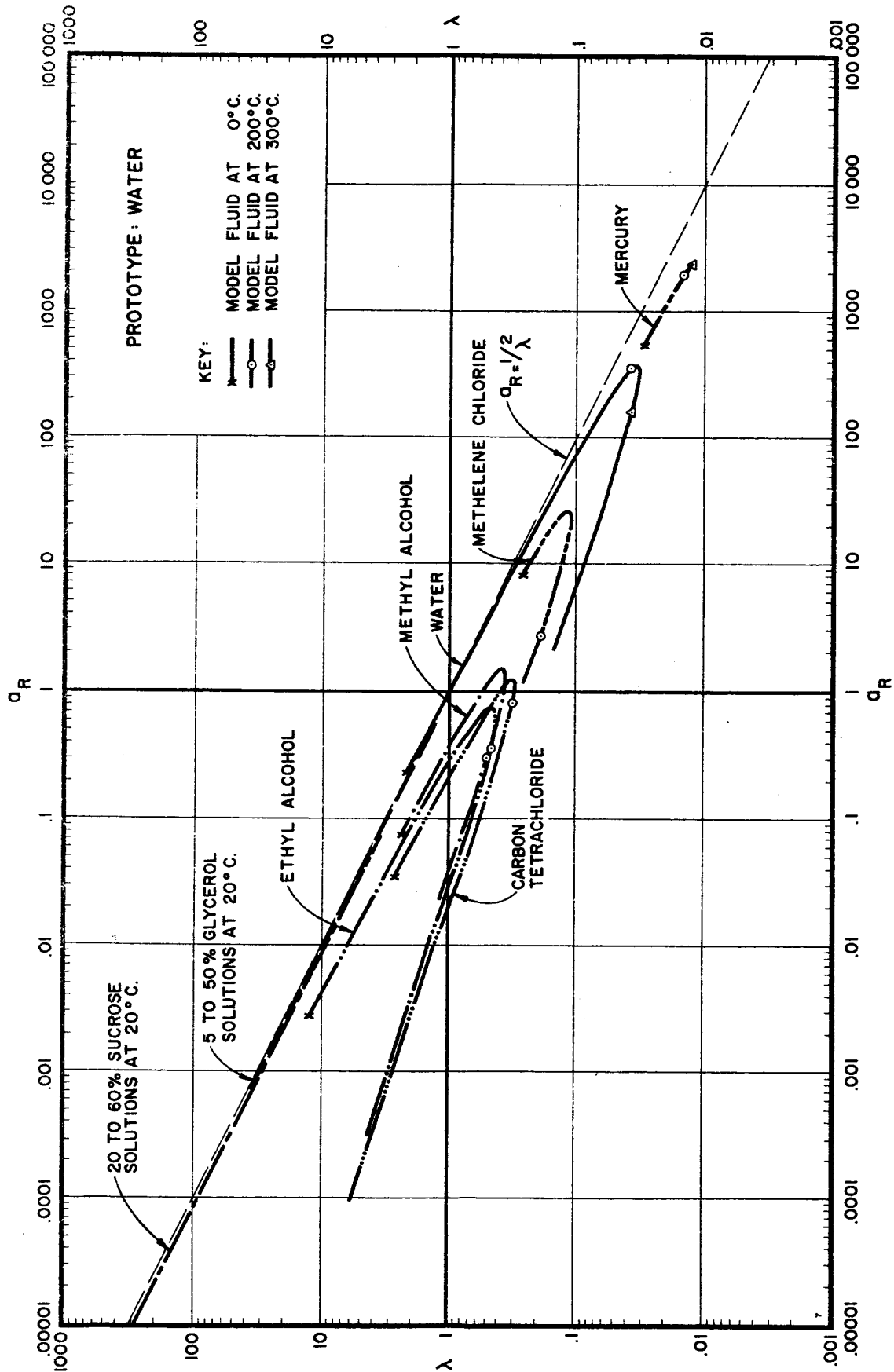


FIGURE 4. SIMULATION PLOT, PROTOTYPE LIQUID; WATER

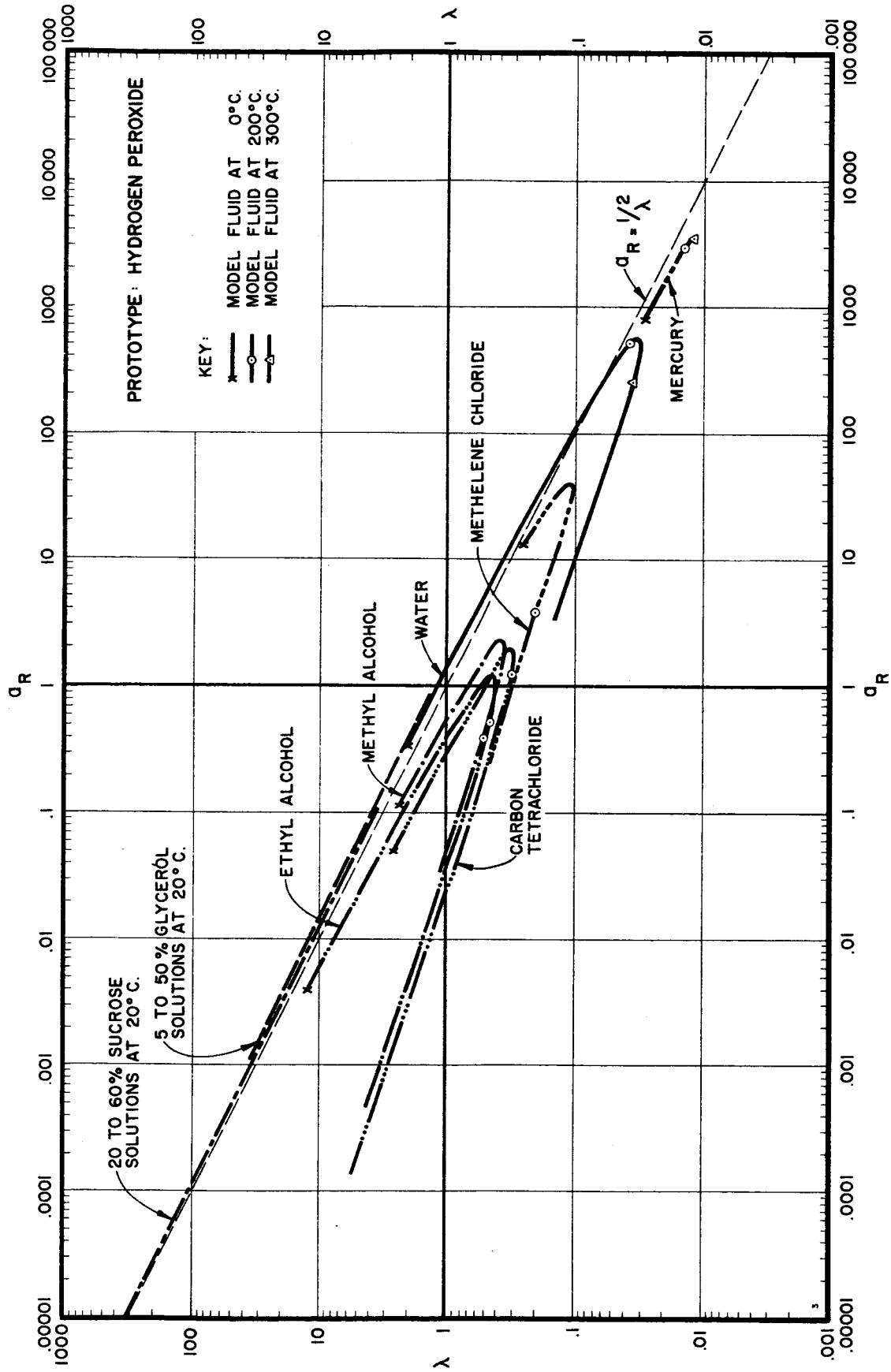


FIGURE 5. SIMULATION PLOT, PROTOTYPE LIQUID; HYDROGEN PEROXIDE

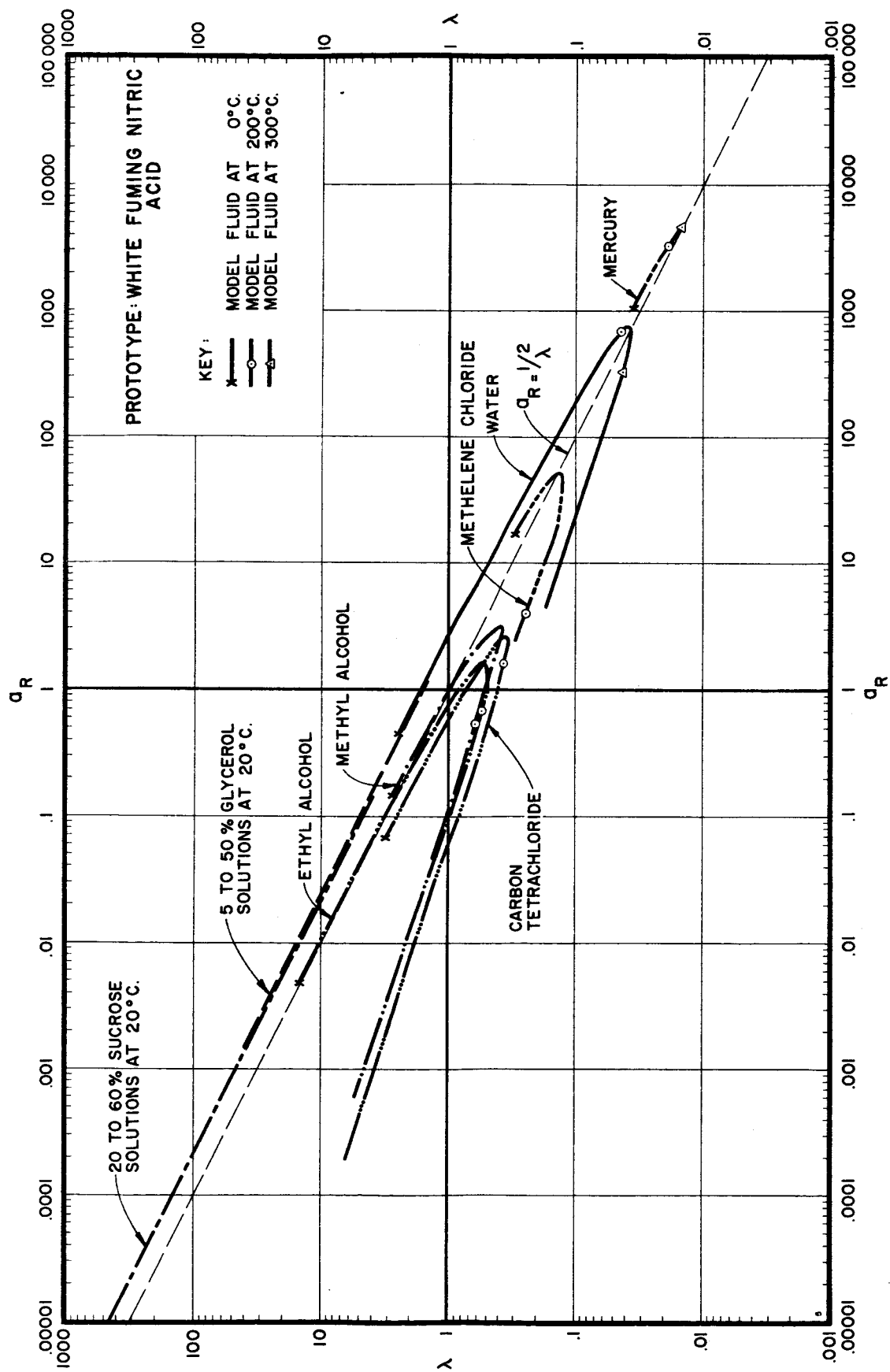


FIGURE 6. SIMULATION PLOT, PROTOTYPE LIQUID; WHITE FUMING NITRIC ACID

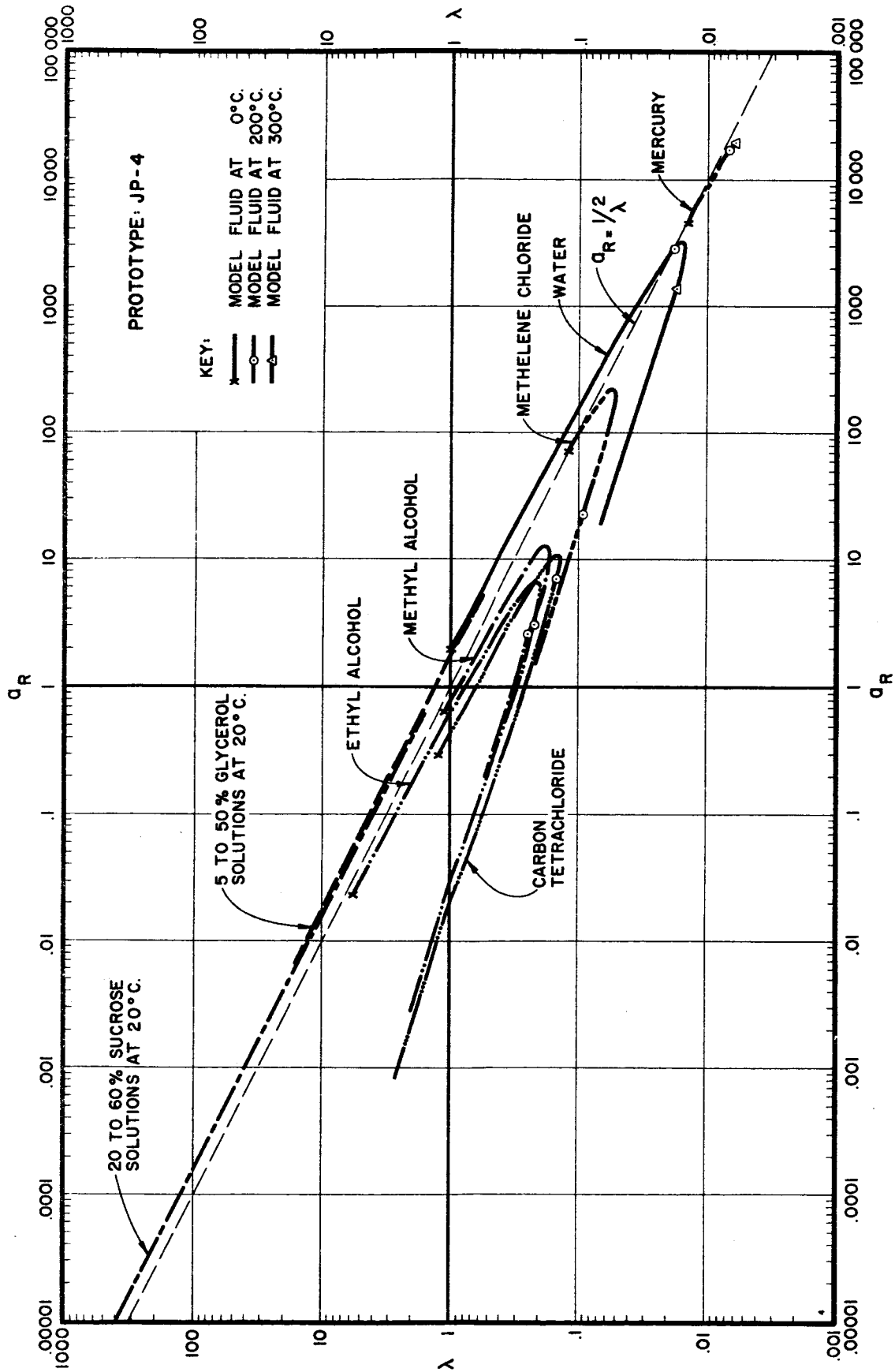


FIGURE 7. SIMULATION PLOT, PROTOTYPE LIQUID; JP-4

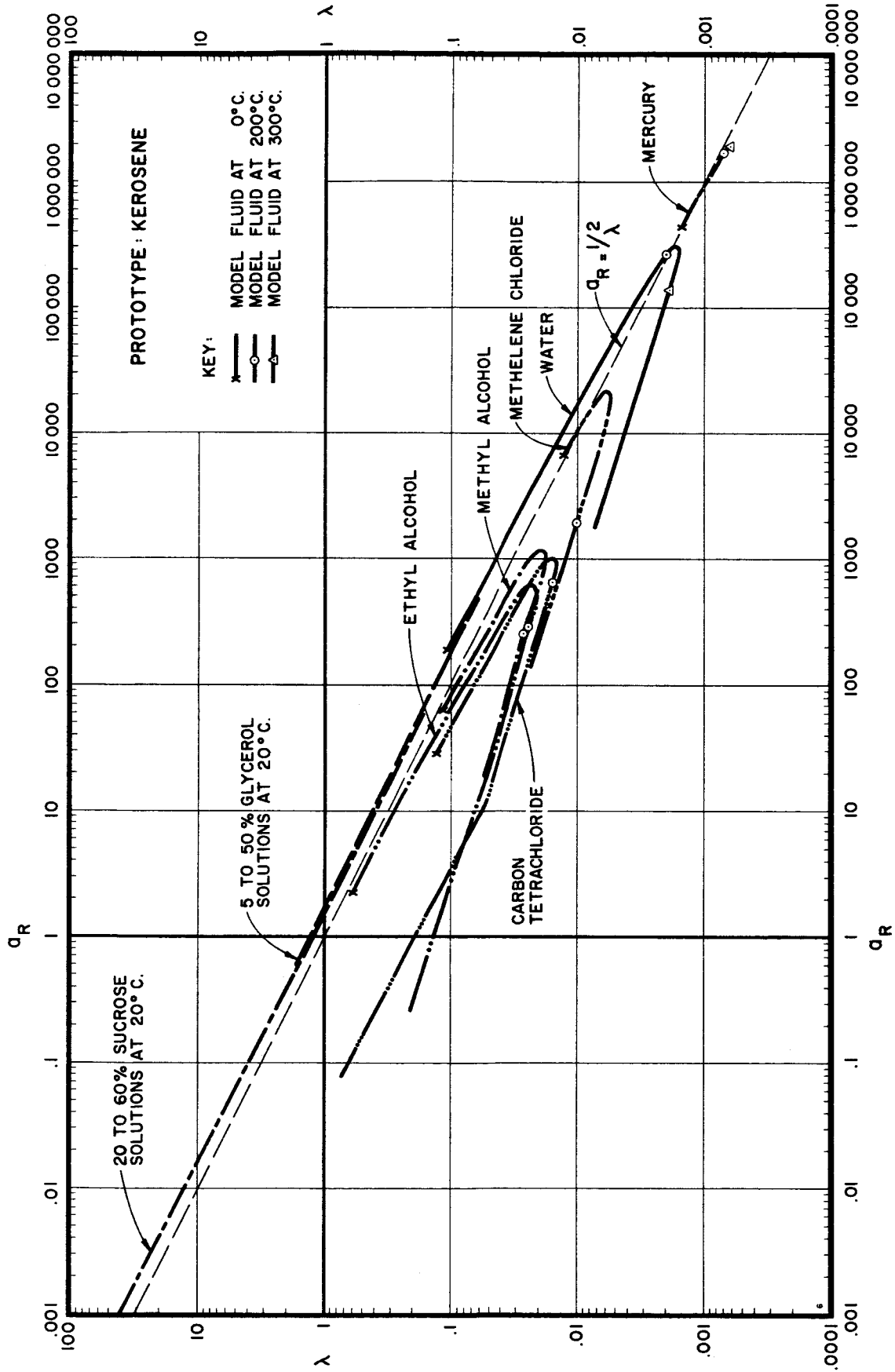


FIGURE 8. SIMULATION PLOT, PROTOTYPE LIQUID; KEROSENE

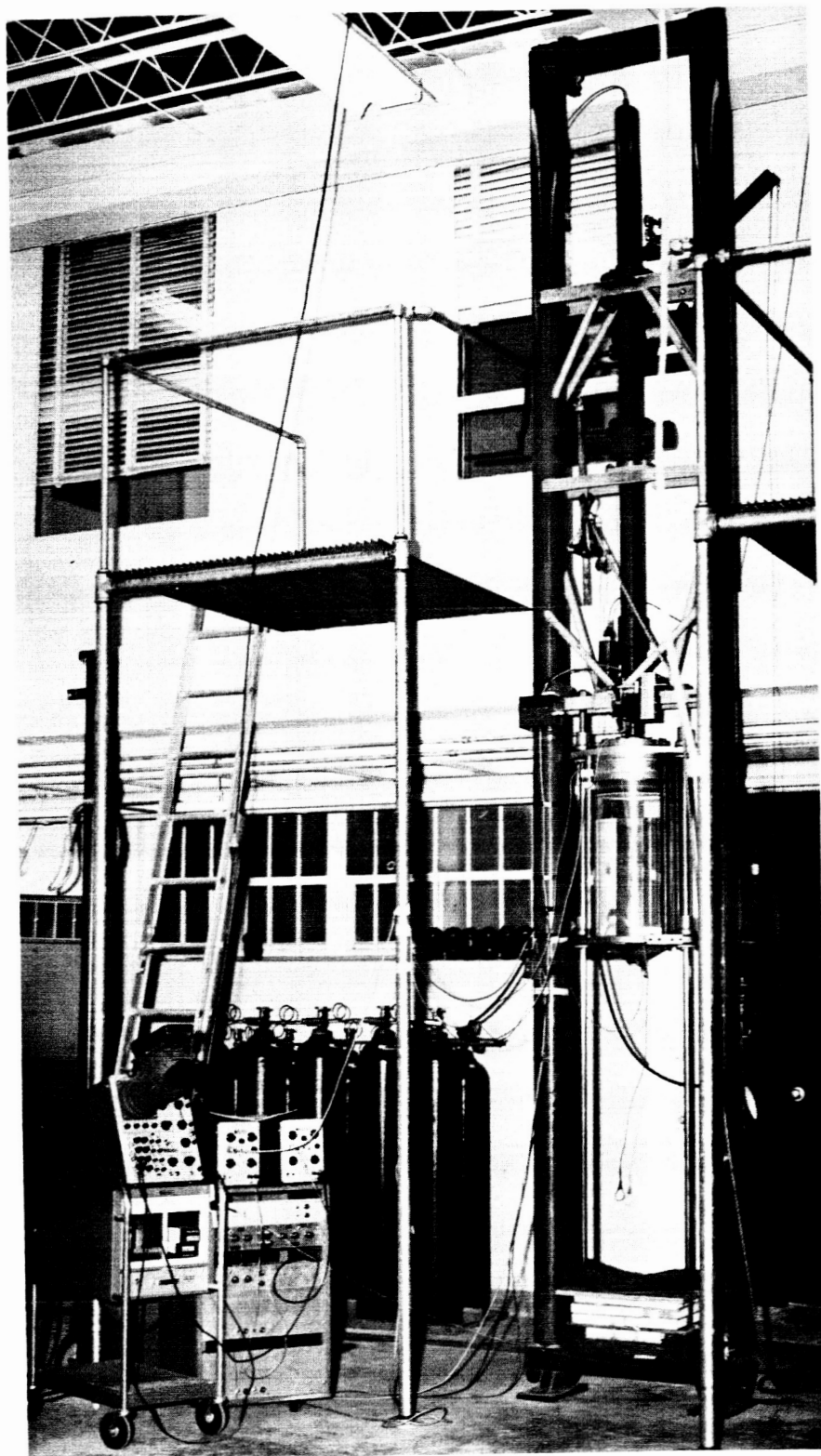


FIGURE 9. TEST FACILITY

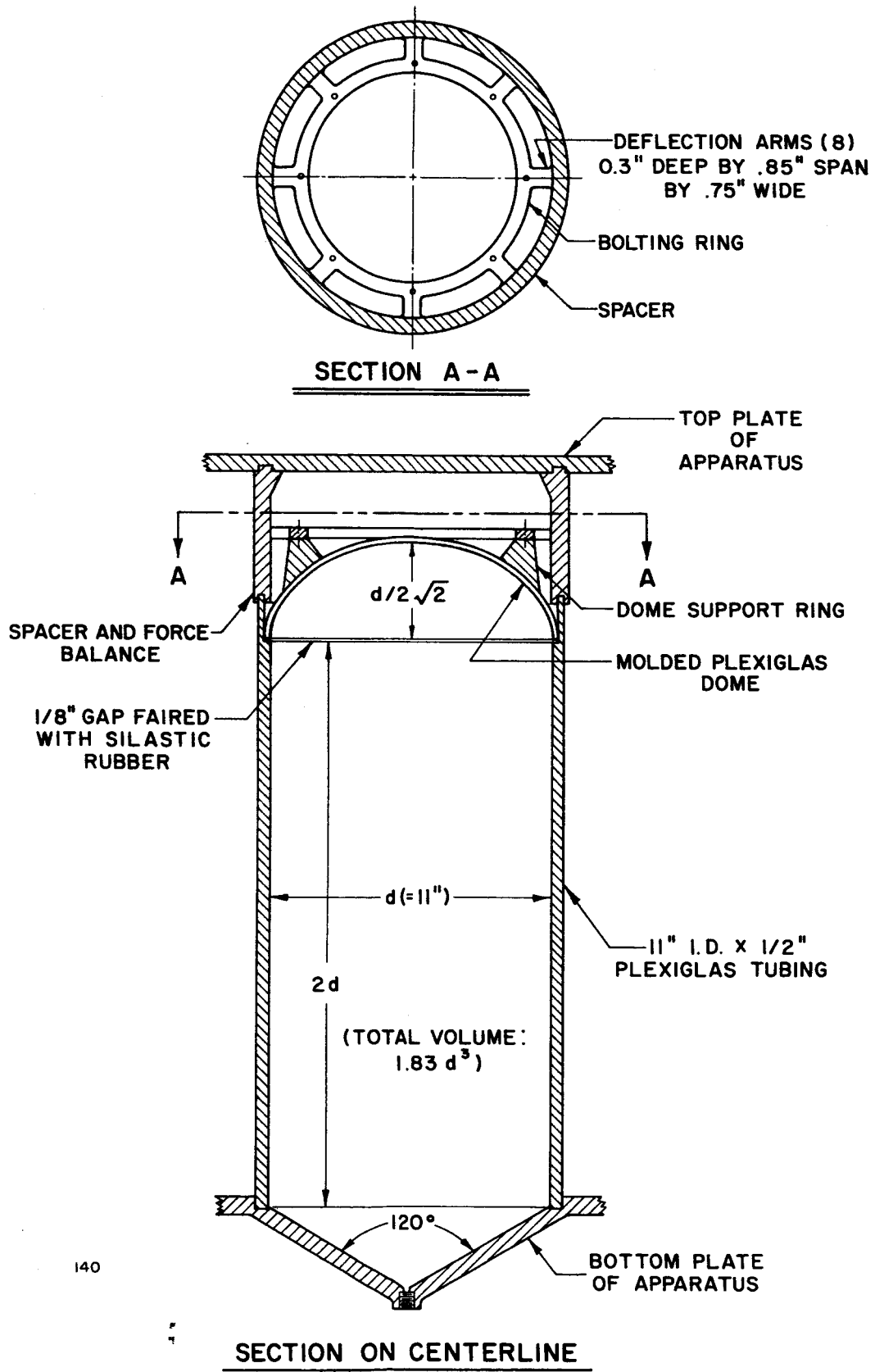
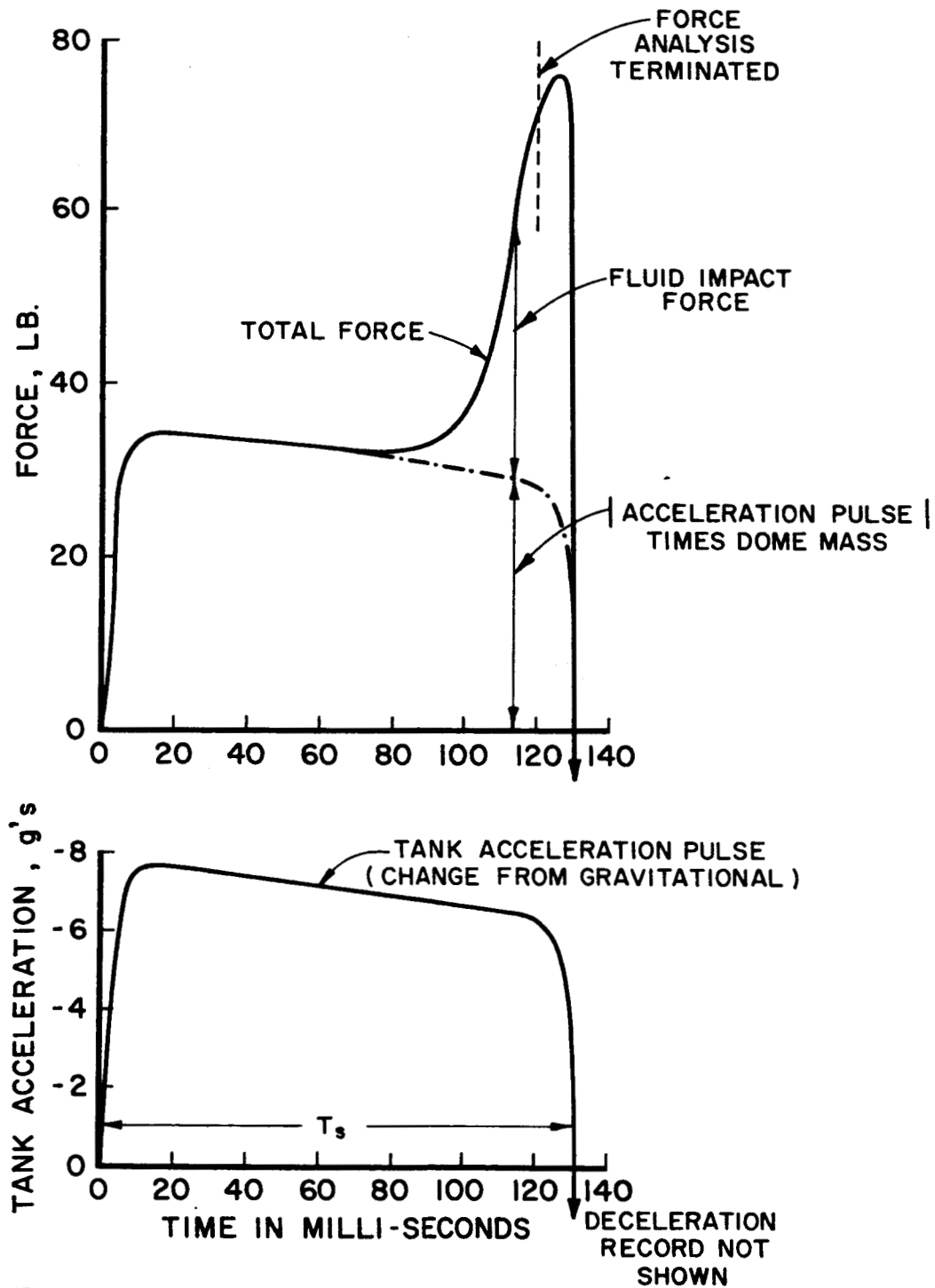


FIGURE 10. TANK AND ASSOCIATED FORCE BALANCE



138

FIGURE 11. TYPICAL TEST RECORD EXPANDED TO ENGINEERING UNITS

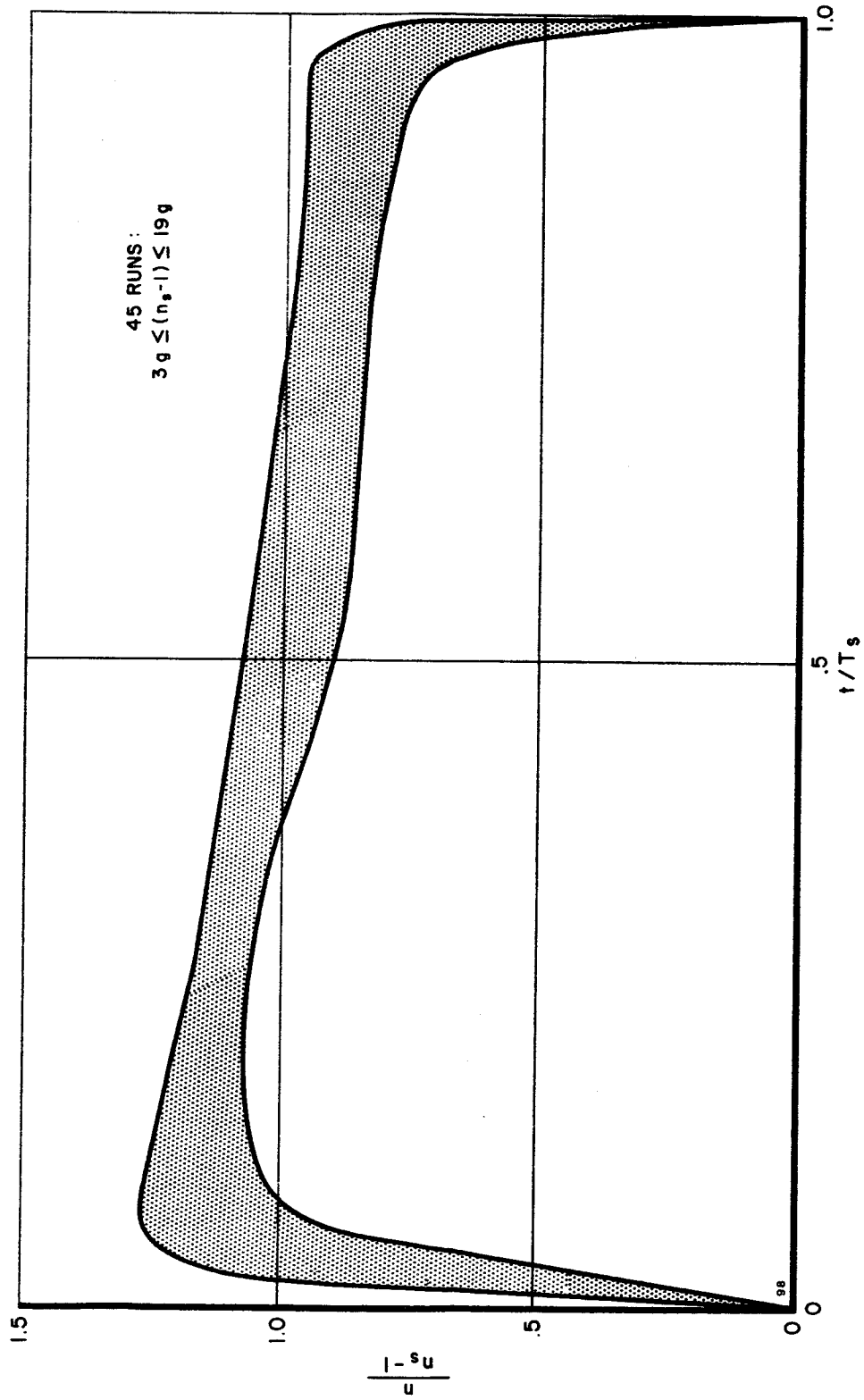


FIGURE 12. NORMALIZED ACCELERATION PULSES

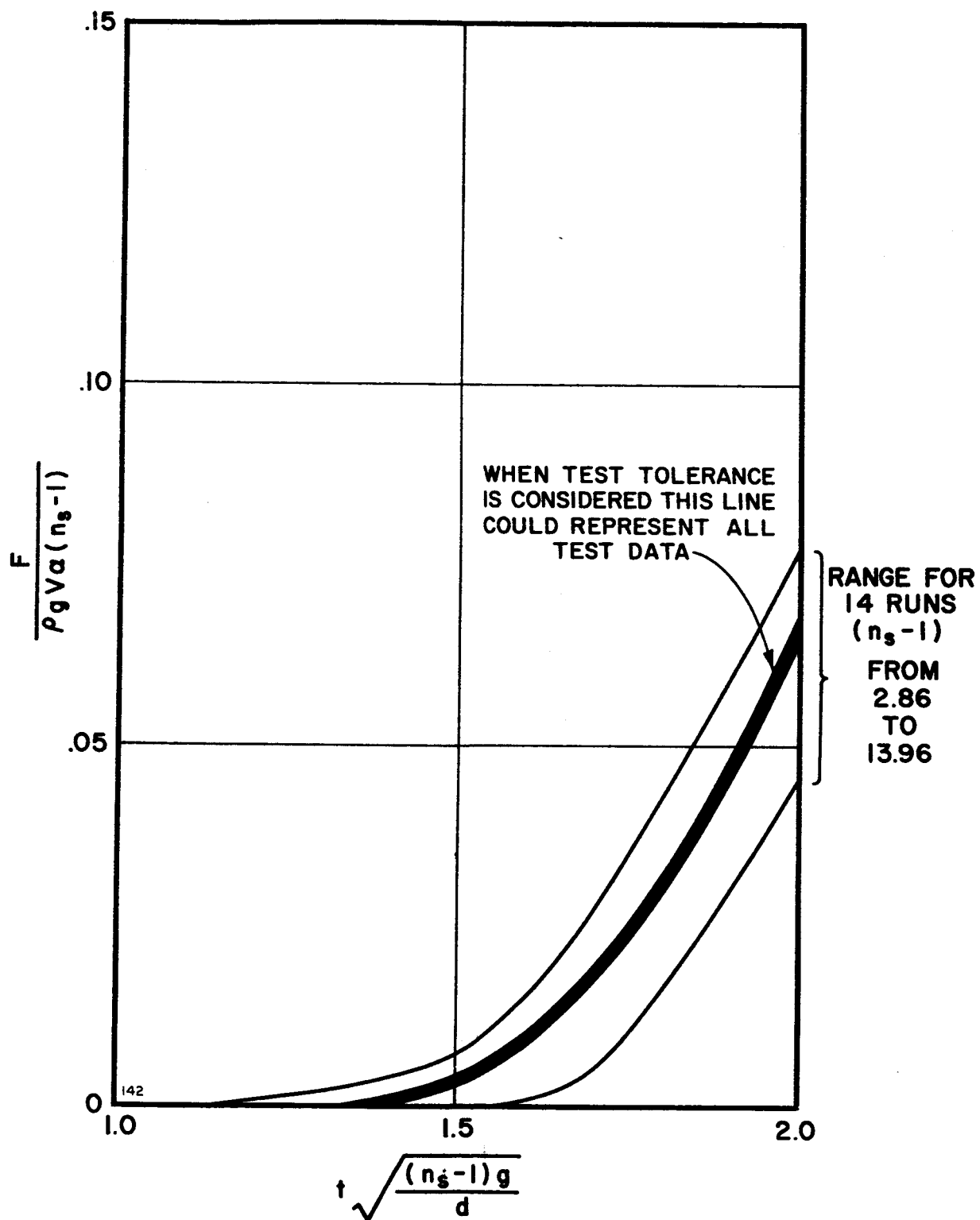


FIGURE 13. NORMALIZED INITIAL IMPACT FORCES,  
TEST FLUID: WATER

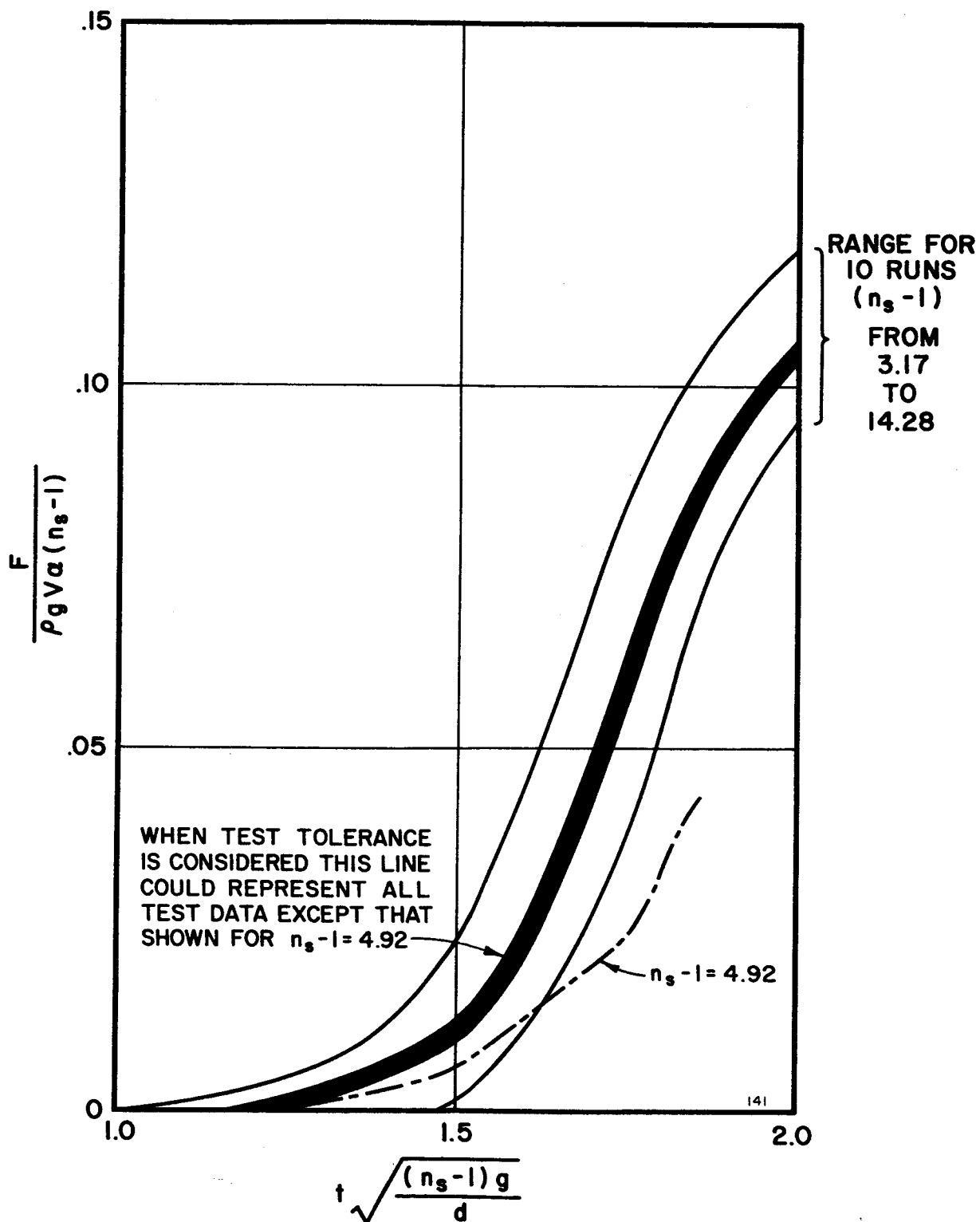


FIGURE 14. NORMALIZED INITIAL IMPACT FORCES,  
TEST FLUID: 30% GLYCEROL

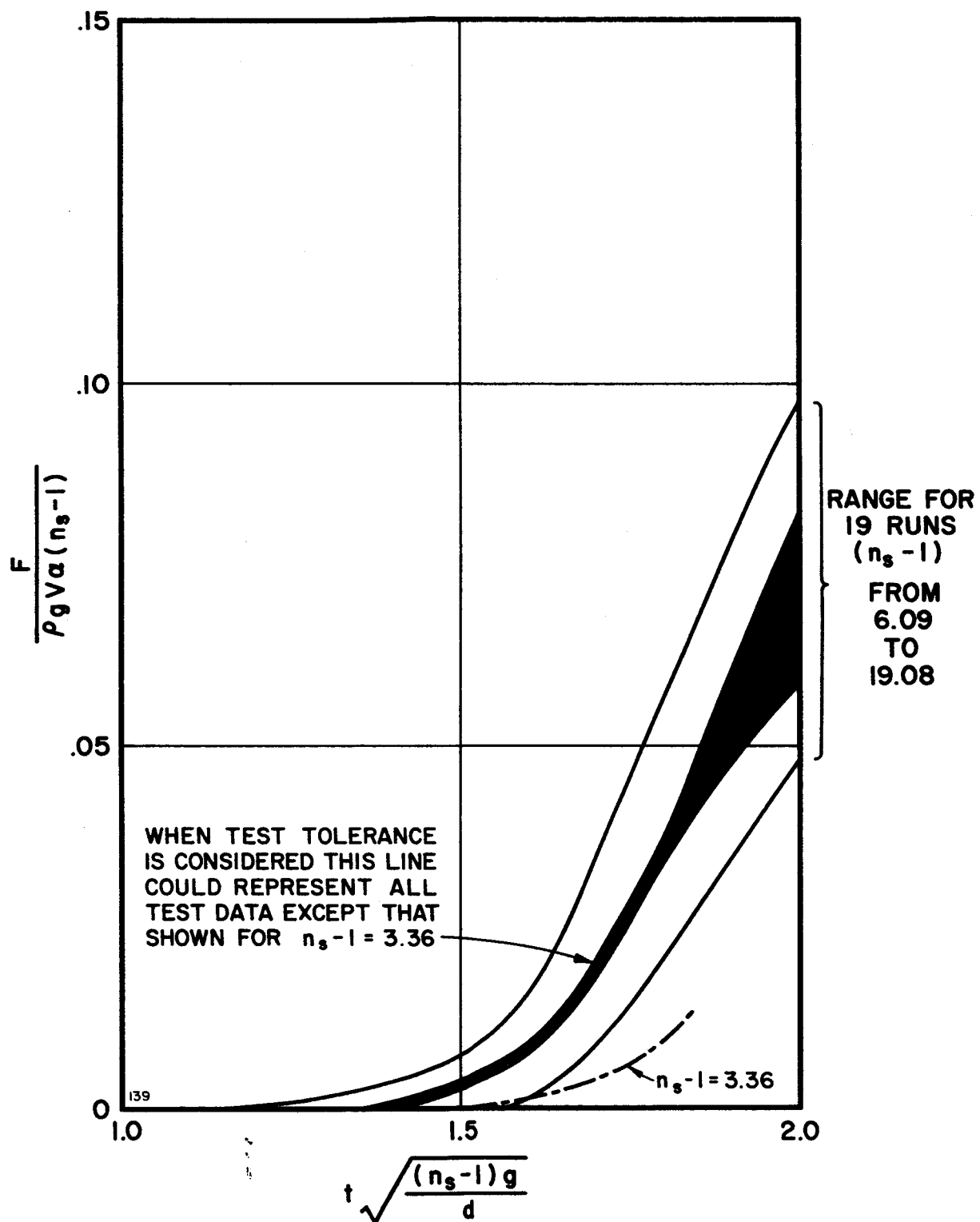


FIGURE 15. NORMALIZED INITIAL IMPACT FORCES, TEST FLUID: METHYL ALCOHOL

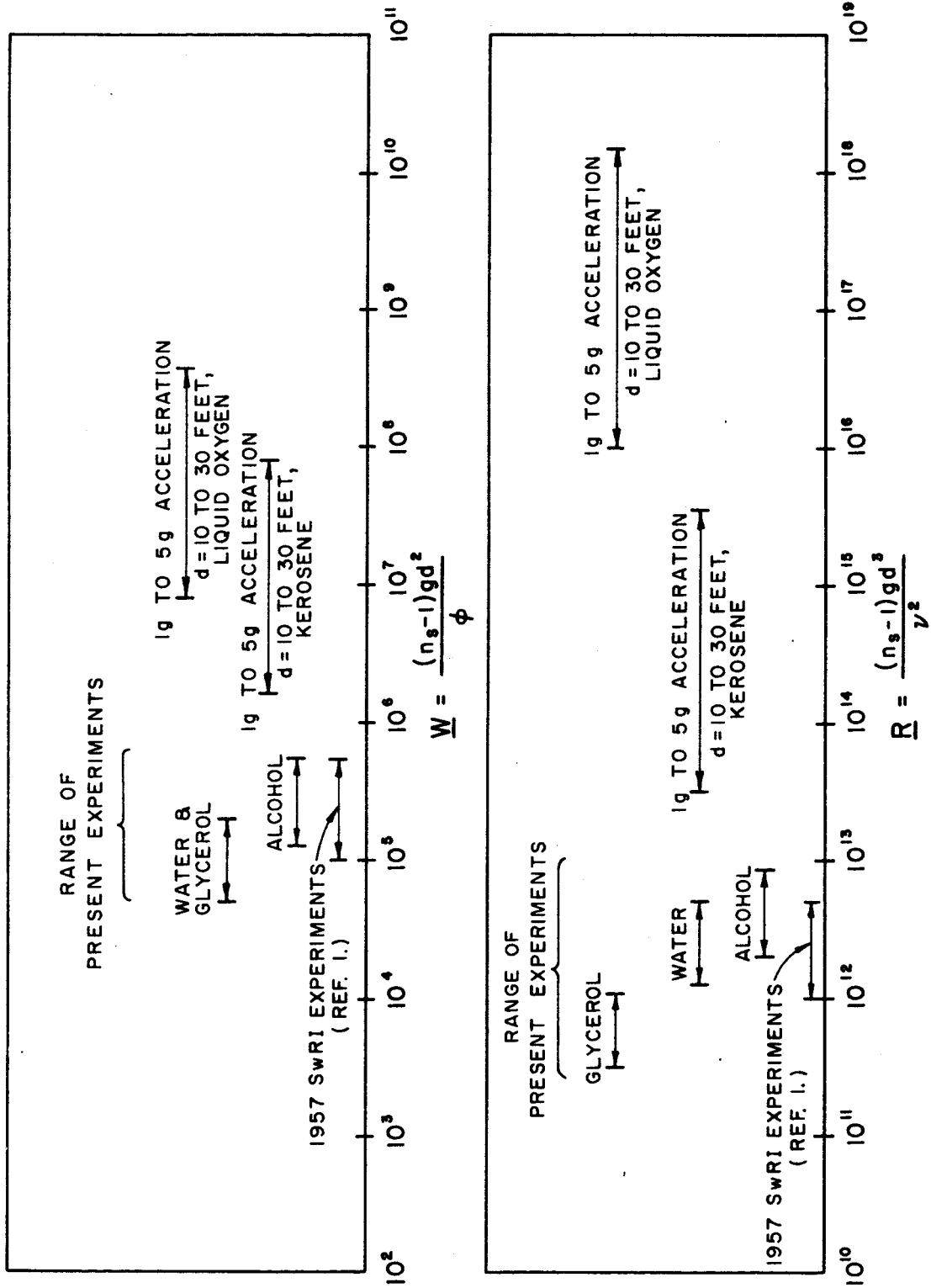


FIGURE 16. MODEL AND PROTOTYPE "REYNOLDS" AND "WEBER" NUMBER RANGES

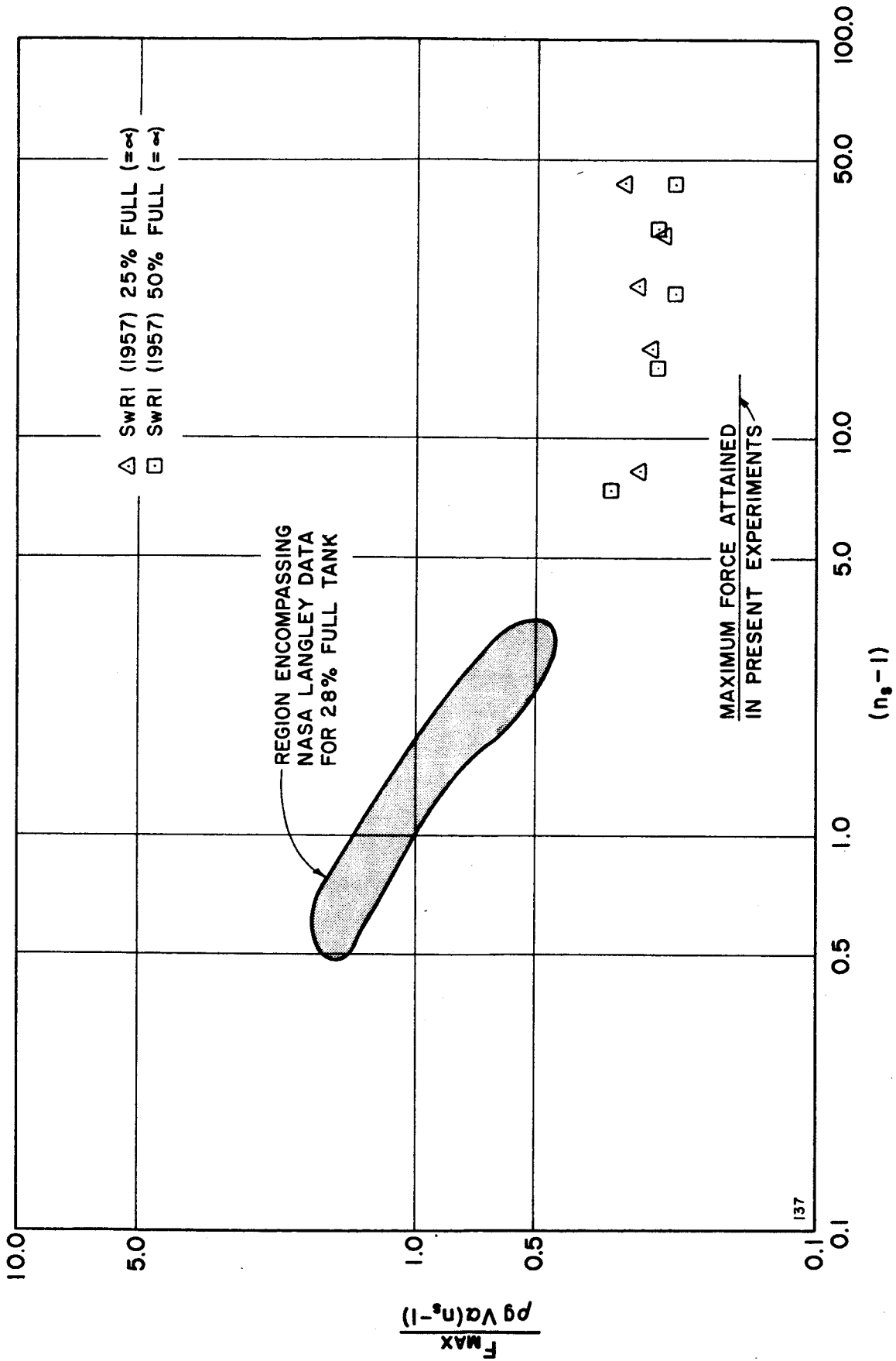


FIGURE 17: COMPARISONS WITH PREVIOUS IMPACT DATA